

EXPERIMENTS ON WEAK INTERACTIONS AT HIGH ENERGIES

BY G. MYATT

Department of Nuclear Physics, University of Oxford*

(Presented at the XIV Cracow School of Theoretical Physics, Zakopane, June 15-28, 1974)

In these lectures one discusses recent experiments on deep inelastic neutrino processes, quasi-elastic reactions, and neutral currents.

DEEP INELASTIC NEUTRINO PROCESSES

I. This lecture will be devoted to a discussion of reactions of the type

$$\nu_{\mu} + N \rightarrow \mu^{-} + X,$$

$$\bar{\nu}_{\mu} + N \rightarrow \mu^{+} + X',$$

where N is a nucleon in a nucleus and X includes all possible final hadronic states. These are so-called charged current reactions. Neutral current reactions will be covered in a later lecture. I will discuss the present situation with respect to the following topics:

Neutrino total cross-sections

Antineutrino/Neutrino cross-section ratio

Distributions in the scaling variable $y = \nu/E$ and in Q^2

Structure factors

Sum rules

II. Neutrino Total Cross-sections

The data here come from three experiments:

The Gargamelle experiment at CERN

The Harvard-Pennsylvania-Wisconsin-NAL experiment at NAL

The Cal-Tech-NAL experiment at NAL

* Nuclear Physics Laboratory, Department of Nuclear Physics, University of Oxford, Keble Road, Oxford, OX1-3RH, England.

(a) The Gargamelle Experiment

This experiment [1] has been carried out in the Gargamelle heavy liquid bubble chamber filled with freon CF_3Br and operated in a wide-band neutrino beam produced by 26 GeV protons. Events were selected in a fiducial volume of 3m^3 and the neutrino energy was determined by the measurement of all the secondaries observed in the bubble chamber. It was estimated that the muon momentum was measured to $\pm 8\%$ and the hadron energy to $\pm 15\%$. A small correction of on average $(5 \pm 2.5)\%$ was applied to the visible energy for undetected neutrons and γ -rays. In order to reject a background from interactions of incoming charged particles a selection on the net momentum along the neutrino beam direction $P_L > 0.6 \text{ GeV}/c$ was applied and events were rejected if Q^2 was greater than $Q^2_{\text{max}} = 4E/(1+2E/M)$. The numbers of events remaining after these selection criteria are shown in Table I. A small subtraction was made for events containing only hadrons in which one hadron was mistaken for a muon. This is less than 2% for $E > 2 \text{ GeV}$. The antineutrino beam contains an appreciable contamination of neutrinos. The ambiguous events (i.e. those with a muon candidate of each sign) were allocated on the basis of the ambiguous events observed in the essentially pure neutrino beam.

In order to calculate cross-sections it is necessary to know the neutrino flux as a function of energy. This is achieved by measuring in the neutrino shield the muons from the $\pi \rightarrow \mu\nu$

TABLE I

Neutrino										
<i>E</i> GeV	1-2	2-3	3-4	4-5	5-6	6-7	7-8	8-9	9-10	10
ν events	723	599	324	115	74	40	32	20	26	9
$\bar{\nu}$ events	134	197	90	64	27	21	11	9	14	5
$\bar{\nu}\nu$ events	44	24	10	9	2	3		1	1	1
Hadronic events	78	34	13	7	5					
Estimated hadronic contamination in ν events	14.6	5.3	2.3			1.2				
Final total of ν events	842	791	411	179	101	60	43	29	40	14

Antineutrino										
<i>E</i> GeV	1-2	2-3	3-4	4-5	5-6	6-7	7-8	8-9	9-10	10
$\bar{\nu}$ events	313	280	130	69	27	12	6	0	2	1
ν events	34	24	17	4	6		1			
$\bar{\nu}\nu$ events	42	48	28	12	8	4	4	3		
Estimated ν in $\bar{\nu}\nu$ events	5.8	8.7	4.1	2	1.9		0.24			
Hadronic events	44	12	5	1	1					
Estimated hadronic contamination in $\bar{\nu}$ events	13	5.5	0.3	1.5						
Final total of $\bar{\nu}$ events	336	314	154	78	33	16	10	3	2	1

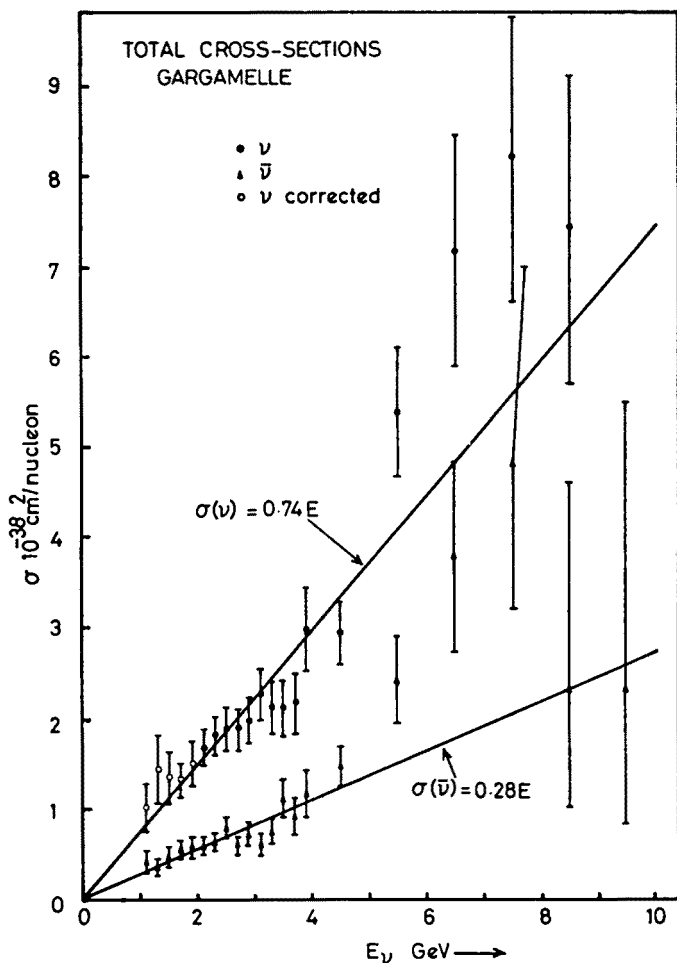


Fig. 1. Total cross-sections for neutrinos and antineutrinos on nucleons as measured by the Gargamelle collaboration [1]

and $K \rightarrow \mu\nu$ decays. The absolute fluxes are known to $\pm 9\%$ in the range 2–6 GeV and $\pm 12\%$ for $E > 6$ GeV. Below 2 GeV the flux can only be obtained by extrapolation of the muon measurements and in fact the total cross-sections have been normalized in this region to the elastic cross-section, which is fairly well known, using the observed events $\nu n \rightarrow \mu^- p$.

The results are shown in Fig. 1. It can be seen that in the range 1–10 GeV both ν and $\bar{\nu}$ cross-sections appear to rise linearly. Straight line fits give for $E > 2$ GeV

$$\sigma_{\nu} = (0.74 \pm 0.03)E \times 10^{-38} \text{ cm}^2/\text{nucleon},$$

$$\sigma_{\bar{\nu}} = (0.27 \pm 0.01)E \times 10^{-38} \text{ cm}^2/\text{nucleon},$$

where E is in GeV.

(b) The Harvard-Pennsylvania-Wisconsin-NAL Experiment [2]

The apparatus is shown in Fig. 2. The detector consists of approximately 60 tons of liquid scintillator which act as a calorimeter. Muons are detected and their signs and momenta determined in a magnetized iron muon spectrometer. Using the pulse height

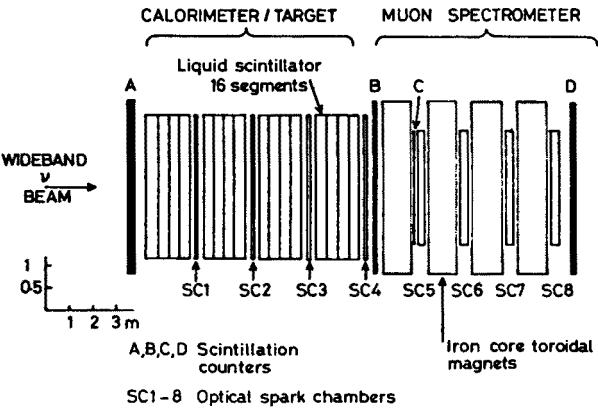


Fig. 2. The apparatus used in the experiment of Benvenuti et al. [2]

from the calorimeter and the muon momentum, the total energy i.e. the neutrino energy E is known to a precision of $\pm 20\%$.

The apparatus was operated in a wide band unfocussed neutrino beam generated by protons of 300 and 400 GeV. The flux of neutrinos was estimated from particle production

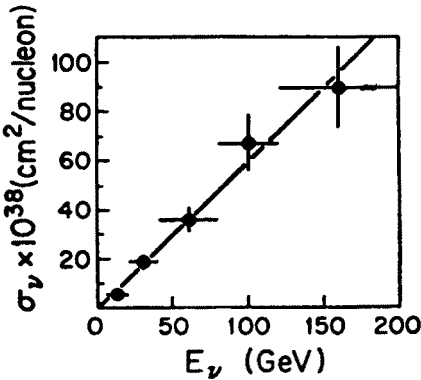


Fig. 3. Neutrino-nucleon total cross-section as measured by Benvenuti et al. [2]

data and the model of Grote, Hagedorn and Ranft [3]. However absolute cross-sections were normalized using 13 observed elastic and low-mass resonance production events i.e. ($Q^2 < 1 \text{ (GeV/c)}^2$, $W^2 < 3.5 \text{ (GeV/c}^2\text{)}^2$) for which a cross-section of $(1.0 \pm 0.3) \times 10^{-38} \text{ cm}^2$ was taken from low energy data.

The results based on 223 neutrino events are shown in Fig. 3. The cross-sections

are consistent with a linear rise up to 200 GeV and a fit gives

$$\sigma_v = (0.58 \pm 0.25) E \times 10^{-38} \text{ cm}^2/\text{nucleon}.$$

This is in good agreement with the linear fit below 10 GeV.

(c) The Cal-Tech-NAL Experiment [4]

The apparatus used is shown in Fig. 4. Events are detected in a calorimeter consisting of iron plates, spark chambers and scintillation counters. The fiducial mass is ~ 85 tons.

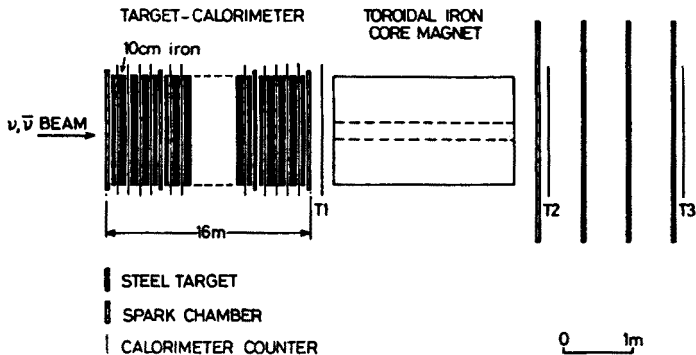


Fig. 4. The apparatus used in the experiment of Barish et al. [4]

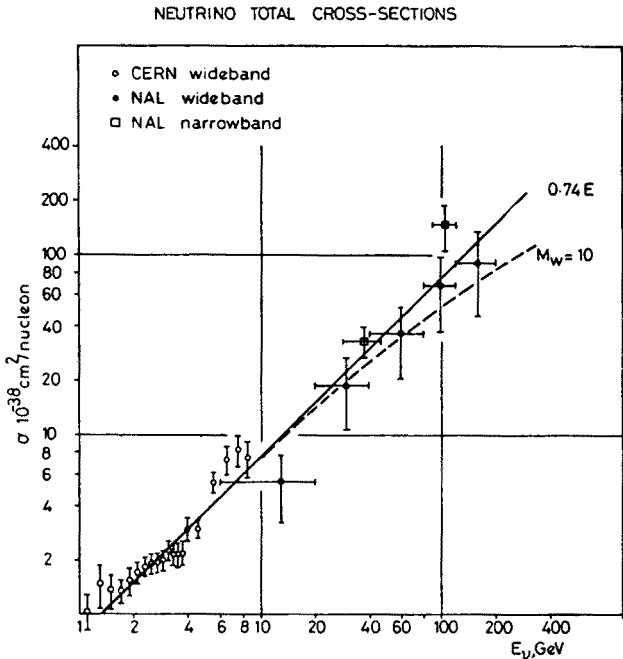


Fig. 5. A compilation of the available data on the neutrino nucleon total cross-section from the three experiments CERN wideband [1], NAL wideband [2] and NAL narrow band [4]. The straight line is the fit to the Gargamelle data [1] in the range 2-10 GeV. The dashed line indicates the deviation which would be introduced by the propagator of an intermediate vector boson of mass 10 GeV

The muons are detected and measured in a magnetized iron muon spectrometer and the neutrino energy can be estimated from the measured muon momentum and the pulse height in the calorimeter.

However the distinctive feature of this experiment is that it is operated in a dichromatic neutrino beam. Pions and kaons of momentum 120 GeV/c are transported along the decay tunnel and the $K \rightarrow \mu\nu$ and $\pi \rightarrow \mu\nu$ decays respectively result in a fairly narrow band of neutrino energies near that of the kaons and a broader band at less than half that energy. Using this beam 621 events were observed at an energy of 38 ± 8 GeV in the pion neutrino peak and 406 events at 106 ± 12 GeV in the kaon neutrino peak. The neutrino flux is obtained by monitoring the particle flux in the decay tunnel.

The results of this experiment are shown in Fig. 5 which also shows all the present data on the neutrino-nucleon cross-section. One may conclude tentatively that the data do not suggest any fall-off of the linear rise up to 160 GeV. Using the coefficient established by the Gargamelle experiment would indicate that $M_W \gtrsim 10$ GeV in a boson propagator damping factor $(1 + Q^2/M_W^2)^{-2}$.

III. The Total Cross-section Ratio $\sigma_{\bar{\nu}}/\sigma_{\nu}$

(a) The Gargamelle Experiment

In Fig. 6 is shown the ratio $R = \sigma_{\bar{\nu}}/\sigma_{\nu}$ as determined in this experiment over the energy range 1–10 GeV. It should be noted that the flux ratio $\Phi_{\bar{\nu}}/\Phi_{\nu}$ is better known than the absolute fluxes themselves and is estimated to have an error of only $\pm 4\%$. It can be seen that R appears to be constant over the energy range and the average value between 2 and 10 GeV is $R = 0.38 \pm 0.02$.

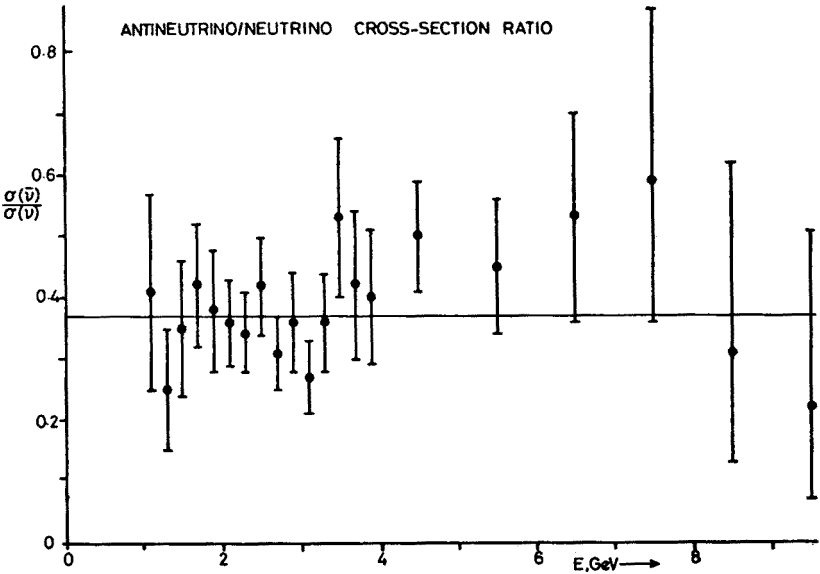


Fig. 6. The ratio $R = \sigma_{\bar{\nu}}/\sigma_{\nu}$ as measured in the Gargamelle experiment [1] as a function of neutrino energy

(b) The Harvard-Pennsylvania-Wisconsin-NAL Experiment [2]

Using events occurring in the calorimeter, and for which therefore the neutrino energy is measured, the cross-section ratio R was determined as a function of energy. This is shown in Fig. 7(a) where it is expressed as the ratio of the coefficients of the linear rise of the

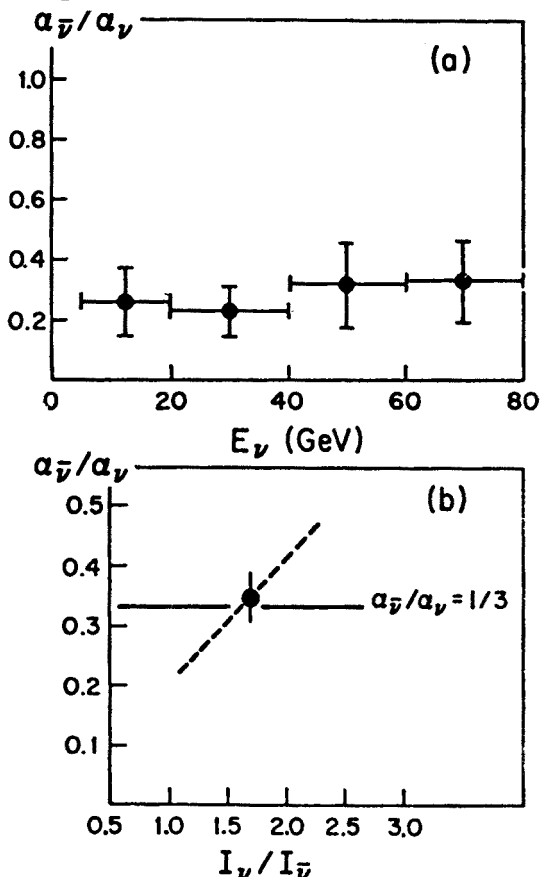


Fig. 7. (a) The ratio $R = \alpha_{\bar{\nu}}/\alpha_{\nu}$ as measured by Benvenuti et al. [2]; (b) The dependence of R upon the weighted flux ratio $I_{\nu}/I_{\bar{\nu}}$

cross-section. This is done to take account of the cross-section and neutrino flux variation across the relatively large energy bins. Above 70 GeV the neutrinos from kaon decay dominate and the flux uncertainty is larger.

In order to increase the statistics, events were also used which occurred in the first section of the iron magnet, and they were assumed to have the same energy distribution as those which occurred in the calorimeter. The result was

$$\frac{\alpha_{\bar{\nu}}}{\alpha_{\nu}} = 0.34 \pm 0.03,$$

where the error is purely statistical. However, this result depends sensitively on the neutrino and antineutrino fluxes predicted by the particle yield formula. Fig. 7(b) shows the depend-

ence of $\alpha_{\bar{\nu}}/\alpha_{\nu}$ on $I_{\nu}/I_{\bar{\nu}}$ where $I = \int \Phi(E)E dE$. Folding in the error on $I_{\nu}/I_{\bar{\nu}}$ we find

$$\frac{\alpha_{\bar{\nu}}}{\alpha_{\nu}} = 0.34 \pm 0.13.$$

If we write the differential cross-section in terms of the variables $x = Q^2/2M\nu$, $y = \nu/E$ where Q^2 is the (four momentum transfer)² and ν is the energy transfer to the nucleon

$$\frac{d^2\sigma_{\nu(\bar{\nu})}}{dx dy} = \frac{G^2 ME}{\pi} \left\{ F_2(x) \left(1 - y - \frac{Mxy}{2E} \right) + 2xF_1(x)_{(+)} y(1 - y/2) xF_3(x) \right\}. \quad (1)$$

If we define

$$A = \frac{\int_0^1 2xF_1(x)dx}{\int_0^1 F_2(x)dx}, \quad B = \frac{-\int_0^1 xF_3(x)dx}{\int_0^1 F_2(x)dx}$$

then for $E \gg M$ the following conditions apply

$$0 < A < 1, \quad 0 < |B| \leq A.$$

Integrating over x and y we obtain, in the high energy limit

$$\frac{\sigma_{\bar{\nu}}}{\sigma_{\nu}} = \frac{3 + A - 2B}{3 + A + 2B}.$$

Using the Gargamelle value of $R = 0.38 \pm 0.02$ we find

$$0.87 \pm 0.05 \leq A < 1, \quad 0.87 \pm 0.05 \leq B \leq 0.90 \pm 0.04.$$

The value of $\int_0^1 F_2(x)dx$ can be obtained from

$$\sigma_{\nu} - \sigma_{\bar{\nu}} = \frac{G^2 ME}{\pi} \int_0^1 F_2(x)dx \times \frac{2}{3} B,$$

whence

$$0.49 \pm 0.03 \leq \int_0^1 F_2(x)dx \leq 0.51 \pm 0.03.$$

IV. Distributions in the Variable $y = \nu/E$

(a) Gargamelle

If scaling holds then at high neutrino energy the distributions in y should be independent of energy. At the energies involved in the CERN experiment [5] this is found not to be the case because of the significant contribution of elastic or resonance production channels and also because of the kinematic limit

$$y_{\max} = \left(1 + \frac{Mx}{2E} \right)^{-1}.$$

However, it is possible to study the y distributions for events in the "scaling region" as

ν -DISTRIBUTIONS FOR EVENTS IN THE SCALING REGION

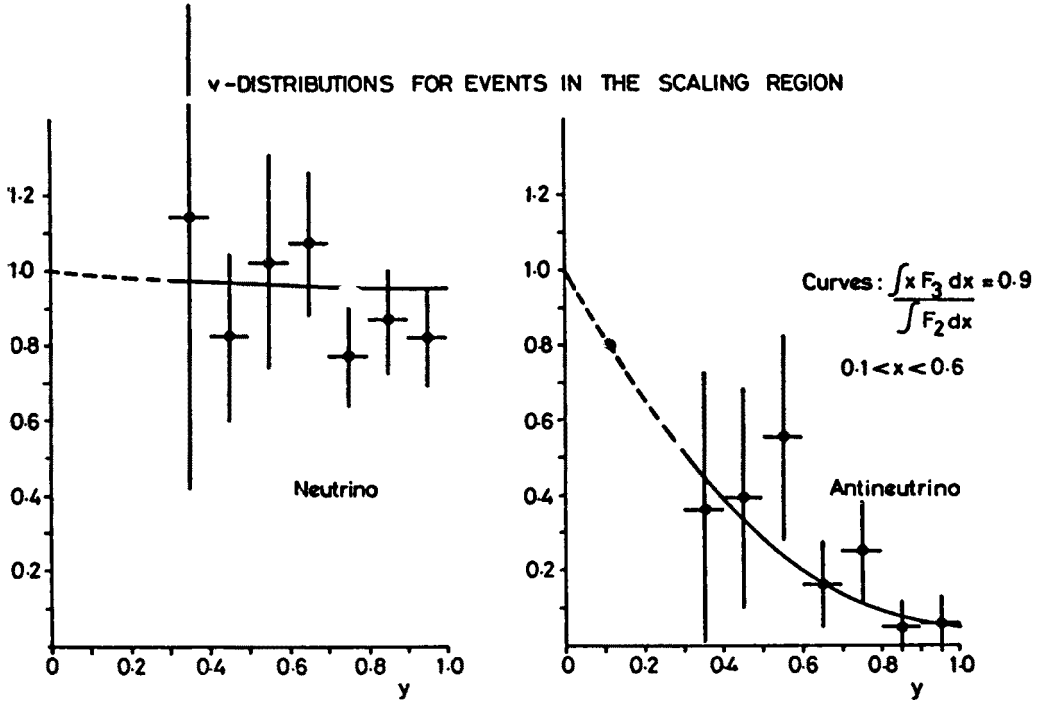


Fig. 8. Distributions in the variable y from the Gargamelle experiment [5] calculated from events in the scaling region $Q^2 > 1 (\text{GeV}/c)^2$, $W^2 > 4(\text{GeV}/c^2)^2$

defined at SLAC i.e. $Q^2 > 1 (\text{GeV}/c)^2$, $W^2 > 4 (\text{GeV}/c^2)^2$. These cuts leave 232 ν and 42 $\bar{\nu}$ events. The double differential cross-section is then evaluated as:

$$\frac{1}{E} \frac{d^2\sigma}{dx dy} = \alpha \frac{d^2N}{N},$$

where α is the coefficient of the linear rise of the total cross-section, and N is the number of events which can contribute i.e. for which x and y lie within the scaling criteria.

This procedure gives the y -distributions shown in Fig. 8 for ν and $\bar{\nu}$. It can be seen that within the large experimental errors the distributions are consistent with the scaling formulae using a value of B derived from the total cross-section ratio.

(b) The Cal-Tech-NAL Experiment [4]

The y -distribution of 1027 neutrino events is shown in Fig. 9. Also shown is the expected distribution if the true y distribution were flat i.e. $A = B = 1$. The rapid fall-off of the data with y is due to the limited angular acceptance of the apparatus.

A detailed study shows that within the range $0 < y < 0.6$, where the experimental efficiency is sufficiently well known, there is no departure from the expectation. This can be expressed quantitatively by fitting an expression of the form $dN/dy = 1 + a(1-y)^2$ to the data. It is found that

$$a = +0.05^{+0.025}_{-0.017}.$$

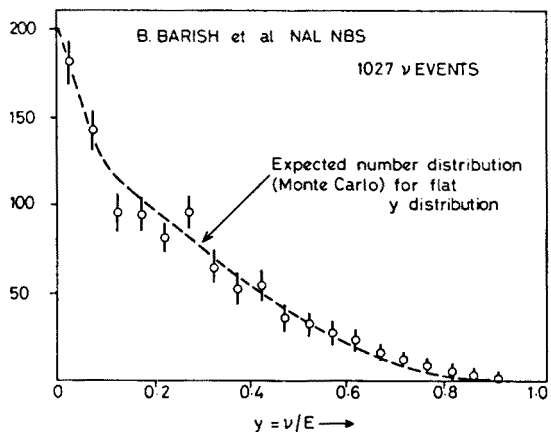


Fig. 9. The distribution in y of 1027 neutrino events from the Cal. Tech.-NAL experiment [4]. The curve shows the distribution expected if the differential cross-section is flat in y

Since $B = (1-a)/(1+a)$, this is equivalent to

$$B = 0.90 \pm 0.36$$

which is consistent with the value obtained in Section III from the total cross-section ratio.

V. The Distribution in Q^2

Since $Q^2 = 2MxyE$, a consequence of scaling is that the average value of Q^2 should increase linearly with energy. This has indeed been found to be the case at CERN [1] in the energy range 1–10 GeV. It is important to note that this test of scaling does not involve

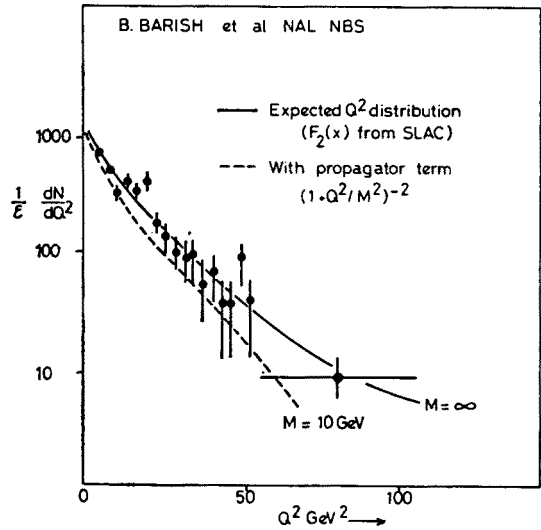


Fig. 10. The corrected Q^2 -distribution of events observed in the Cal. Tech.-NAL experiment. The dashed curve indicates the expected distribution if the weak interaction were mediated by an intermediate vector boson of mass $10 \text{ GeV}/c^2$

any determination of neutrino fluxes. Recently, the Cal-Tech-NAL group have published [4] a Q^2 -distribution extending beyond 50 (GeV/c)². This is shown in Fig. 10 where the data have been corrected for the experimental efficiency ε . The distribution is found to agree with scaling if the distribution in x has the form of $F_2^{ed}(x)$ measured in electroproduction at SLAC. If a scaling breakdown is parametrized as a damping term $(1 + Q^2/M^2)^{-2}$, as for example would be introduced by an intermediate vector boson of mass M , then it is found that

$$M \geq 10.3 \text{ GeV}/c^2, \quad 90\% \text{ C.L.}$$

VI. Structure Factors

Using the method described in Section IV the Gargamelle data have been used to extract structure factors $F_2(x)$, $xF_3(x)$ in the scaling region $Q^2 > 1$ (GeV/c)², $W^2 > 4$ (GeV/c)². If we assume the Callan-Gross [6] relation $2xF_1 = F_2$, which is strongly supported by electroproduction experiments [7], then Eq. (1) yields

$$F_2(x) = \frac{\pi}{G^2 M} \frac{\left[\frac{1}{E} \frac{d^2\sigma_v}{dx dy} + \frac{1}{E} \frac{d^2\sigma_{\bar{v}}}{dx dy} \right]}{2(1 - y + y^2/2)}, \quad (2)$$

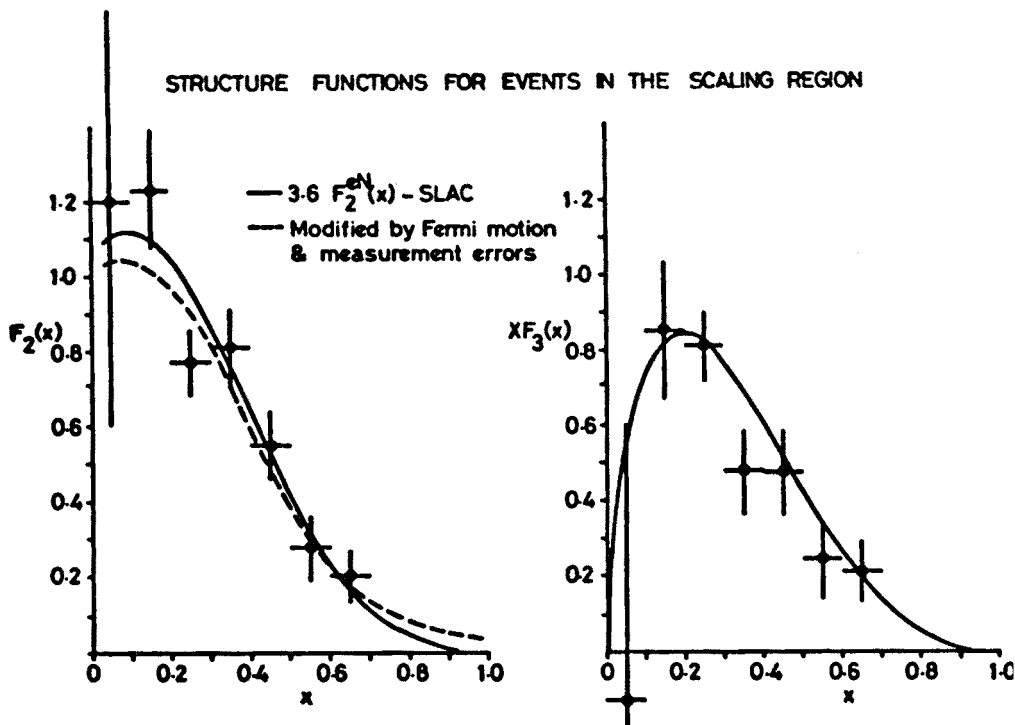


Fig. 11. The structure factors $F_2(x)$ and $xF_3(x)$ as determined from the Gargamelle experiment using only events with $Q^2 > 1$ (GeV/c)², $W^2 > 4$ (GeV/c)²

$$xF_3(x) = \frac{\pi}{G^2 M} \frac{\left[\frac{1}{E} \frac{d^2\sigma_\nu}{dx dy} - \frac{1}{E} \frac{d^2\sigma_{\bar{\nu}}}{dx dy} \right]}{2y(1-y/2)}. \quad (3)$$

The results are shown in Fig. 11. $F_2(x)$ may be compared with $3.6 F_2^{\text{eN}}$, where the factor 3.6 comes from the quark model. The effects of Fermi motion and measurement errors on the shape of F_2 are indicated by the dashed curve. $F_3(x)$ is compared with the prediction of the quark parton model of McElhaney and Tuan [8]. The quark and antiquark momentum distributions were obtained by a fit to electroproduction data. Thus, within errors, the neutrino data are consistent with scaling and with the quark parton model.

VII. Sum Rules

It has been found in the Gargamelle experiment that the distributions in $x = Q^2/2M\nu$ vary with energy over the range 1–11 GeV. However, when plotted in terms of the Bloom-Gilman [9] variable $x' = Q^2/(2M\nu + M^2)$ the distributions appear to be independent of neutrino energy. This suggests that x' is the relevant scaling variable in the low energy region. Taking this point of view one may further assume that the distributions in x' observed at low energies correspond to the x distributions in the scaling region. One is thus able to use data of much greater statistical weight than that remaining after the “scaling” cuts discussed in Section IV. Defining the structure factors $\bar{F}_2(x')$ and $x'\bar{F}_3(x')$ by

$$\bar{F}_2(x') = \frac{3\pi}{4G^2 ME} \left\{ \frac{d\sigma_\nu}{dx'} + \frac{d\sigma_{\bar{\nu}}}{dx'} \right\}, \quad (4)$$

$$x\bar{F}_3(x') = \frac{3\pi}{2G^2 ME} \left\{ \frac{d\sigma_\nu}{dx'} - \frac{d\sigma_{\bar{\nu}}}{dx'} \right\}, \quad (5)$$

the data on $\bar{F}_2(x')$ shown in Fig. 12 are obtained. It can be seen that $\bar{F}_2(x')$ appears to be independent of neutrino energy and is comparable to $3.6 F_2^{\text{eN}}$.

(a) Comparison of $\int F_2(x)dx$ with the Quark Parton Model

If the quarks have isospin 1/2 and the Gell-Mann, Zweig fractional charge assignments then for the $\Delta S = 0$ part of the weak cross-section

$$\frac{\int F_2^{\nu\text{N}} dx}{\int F_2^{\text{eN}} dx} \leq \frac{18}{5} = 3.6.$$

The equality would be fulfilled if the contribution of strange quarks and antiquarks to the electroproduction cross-section were negligible. This is reasonable since the fact that the ratio $\sigma_{\bar{\nu}}/\sigma_\nu$ is near 1/3 means that the contribution of non-strange antiquarks to the total cross-section must be $\lesssim 5\%$.

Using the value of $\int F_2 dx$ obtained in Section III from the total cross-sections and correcting for the small $\Delta S = 1$ contribution and the fact that $n/p = 1.19$ in CF_3Br

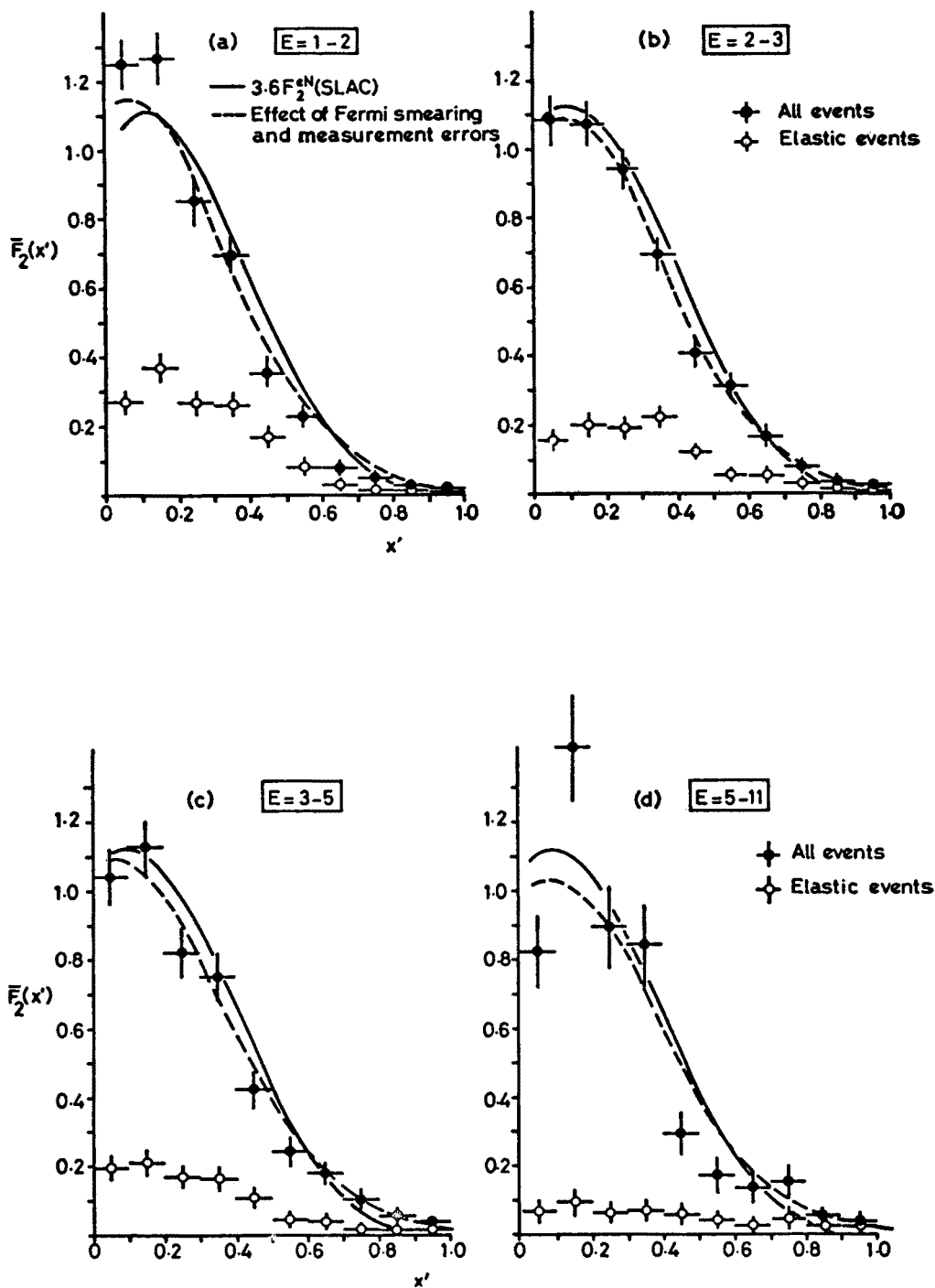


Fig. 12. The structure factor $\bar{F}_2(x')$ as determined from the Gargamelle data: (a) $1 < E < 2$ GeV, (b) $2 < E < 3$ GeV, (c) $3 < E < 5$ GeV, (d) $5 < E < 11$ GeV

one obtains

$$[\int F_2^{vN} dx]_{\Delta S=0}^{n=p} = 0.52 \pm 0.03,$$

and the electroproduction experiments [7] yield

$$\int (F_2^{ep} + F_2^{en}) dx = 0.29 \pm 0.02.$$

Therefore

$$\frac{\int_{\Delta S=0} F_2^{vN} dx}{\int F_2^{eN} dx} = 3.59 \pm 0.31.$$

This result supports the fractional charge assignments of the quarks and in common with the electroproduction data requires $\sim 50\%$ of the nucleon momentum to be carried by inactive constituents (gluons).

(b) The Gross-Llewellyn-Smith Sum Rule [10], The Number of Valence Quarks

This sum rule has the form:

$$\frac{1}{2} \int (F_3^{vn} + F_3^{vp}) dx = 2B + Y - \frac{3}{2} Y \sin^2 \theta_C.$$

For a nucleon target $B = Y = 1$ and the right hand side becomes

$$3(1 - \frac{1}{2} \sin^2 \theta_C) = 2.925$$

It is easy to show that if we neglect the Cabibbo angle θ_C then in the quark parton model the sum rule corresponds to the number of valence quarks in the nucleon, $N - \bar{N} = 3$.

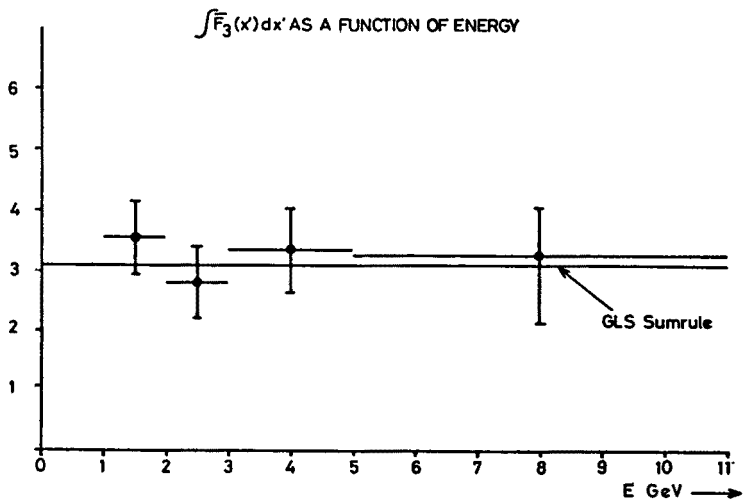


Fig. 13. The value of $\int \bar{F}_3(x') dx'$ from the Gargamelle experiment shown as a function of neutrino energy

Actually in freon $S = n/p = 1.19$ and

$$[\int F_3^{\nu N} dx] = \frac{1}{2} \int (F_3^{\nu n} + F_3^{\nu p}) dx + \left(\frac{S-1}{S+1} \right) \int \frac{dx}{x} (F_2^{\nu n} - F_2^{\nu p}) = 2.925 + 0.17 = 3.1.$$

By the Adler sum rule [11] the second integral equals 2.

$x' \bar{F}_3(x')$ has been extracted from the Gargamelle data using Eq. (5) and the integral over x' performed as a function of neutrino energy. The result is shown in Fig. 13. It can be seen that there is no apparent dependence on energy, again suggesting that the distributions in x' at low energy correspond to those in x at high energy. Using all data between 1 and 11 GeV the result obtained is

$$\int_0^1 \bar{F}_3(x') dx' = 3.2 \pm 0.6.$$

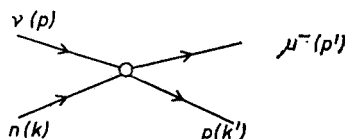
This result again supports the quark-parton model and is independent of the quark charge assignments.

REFERENCES

- [1] T. Eichten et al., *Phys. Lett.* **46B**, 274 (1973).
- [2] A. Benvenuti et al., *Phys. Rev. Lett.* **32**, 125 (1974).
- [3] H. Grote, R. Hagedorn, J. Ranft, CERN-SIS-3000 (1970).
- [4] B. C. Barish et al., Reported at the International Conference on Neutrino Physics and Astrophysics, Philadelphia, 1974.
- [5] H. Deden et al., to be published.
- [6] C. G. Callan, D. J. Gross, *Phys. Rev. Lett.* **22**, 156 (1969).
- [7] A. Bodek et al., *Phys. Rev. Lett.* **30**, 1087 (1973).
- [8] R. McElhaney, S. F. Tuan, *Phys. Rev.* **D8**, 2267 (1973).
- [9] E. Bloom, F. Gilman, *Phys. Rev. Lett.* **25**, 1140 (1970).
- [10] D. J. Gross, C. H. Llewellyn-Smith, *Nucl. Phys.* **B14**, 337 (1969).
- [11] S. L. Adler, *Phys. Rev.* **143**, 1144 (1966).

QUASI ELASTIC REACTIONS

The Reaction $\nu n \rightarrow \mu^- p$



In the current-current V-A theory of weak interactions this process is described by the Hamiltonian

$$H = \frac{G}{\sqrt{2}} \cos \theta_C J_\mu j_\mu^\dagger,$$

where $j_\mu = \bar{u}(p')\gamma_\mu(1+\gamma_5)u(p)$ and the baryonic current has the most general form

$$J_\mu = \bar{u}(k') \left\{ g_V \gamma_\mu - \frac{\mu}{2M} \sigma_{\mu\nu} q_\nu + \frac{ig_S}{m_\mu} q_\mu + \right. \\ \left. + g_A \gamma_\mu \gamma_5 - \frac{g_T}{2M} \sigma_{\mu\nu} q_\nu \gamma_5 + \frac{ig_P}{m_\mu} q_\mu \gamma_5 \right\} u(k), + \\ q = p - p' = k' - k,$$

where the coupling constants will be functions of $Q^2 = -q^2$. The conventional theory tells us something about the coupling constants $g_V - g_P$.

(a) Electron-muon universality says that g_V and g_A are equal to those measured in nuclear β -decay at $Q^2 = 0$ i.e. $g_V = 1$, $g_A = 1.25$

(b) The Conserved Vector Current hypothesis says

$$q_\mu J_\mu^\nu = 0.$$

This can only be true if $g_S = 0$.

(c) The extension of CVC — the isotriplet current hypothesis relates the weak vector current to the isovector part of the electromagnetic current. This identifies $\mu = \mu_p - \mu_n$ (anomalous magnetic moments) and the Q^2 dependence of μ is known from electron scattering.

(d) If the induced pseudoscalar interaction is assumed to be dominated by pion exchange then we find

$$\frac{g_P}{m_\mu} = \frac{f_\pi g_\pi}{m_\pi^2 + Q^2},$$

where f_π is the $\text{pn}\pi$ coupling constant $|f_\pi|^2/4\pi = 15.7$ and g_π is the pion-lepton coupling constant obtained from $\pi \rightarrow \mu\nu$ decay. In the cross-section the induced PS contribution appears multiplied by m_μ^2 , and in addition the form given above results in a rapid fall-off with Q^2 . Hence the PS contribution is typically $< 1\%$.

(e) If we consider the behaviour of the baryon current under the G -parity operation $G = Ce^{i\pi I_2}$ then for the bare currents

$$GJ_\mu^V G^{-1} = J_\mu^V, \quad GJ_\mu^A G^{-1} = -J_\mu^A.$$

If we take the general form for the current then we find that the scalar and tensor terms have opposite G -parity behaviour to the bare currents — they are 2nd class currents (Weinberg). It is not thought reasonable that the G -parity conserving strong-interaction should induce currents with the opposite G -parity behaviour to the bare currents.

Differential Cross-section

If we include all terms but the induced scalar we find

$$\begin{aligned} \frac{d\sigma}{dQ^2} = & \frac{G^2 \cos^2 \theta_C}{32\pi M^2 E^2} \left\{ (Q^2 + m_\mu^2) \left[4M^2(g_A^2 - g_E^2) + (Q^2 - m_\mu^2)(g_A^2 + g_M^2) + \right. \right. \\ & + m_\mu^2 \left(Q^2 \frac{g_P^2}{m_\mu^2} - 4M \frac{g_A g_P}{m_\mu} \right) \left. \right] + 4(s-u) \left[Q^2 g_A g_M - m_\mu^2 g_T \left(g_A + \frac{Q^2 g_P}{2M m_\mu} \right) \right] + \\ & \left. + (s-u)^2 \left[g_A^2 + \frac{4M^2 g_E^2 + Q^2 g_M^2}{4M^2 + Q^2} + \frac{Q^2}{4M^2} g_T^2 \right] \right\}, \end{aligned}$$

where m_μ = muon mass, M = nucleon mass, and $s-u = (k-p')^2 - (k+p)^2 = 4ME - m_\mu^2 - Q^2$. The high energy limit is

$$\lim_{E \rightarrow \infty} \frac{d\sigma}{dQ^2} = \frac{G^2 \cos^2 \theta_C}{2\pi} \left\{ g_A^2 + \frac{4M^2 g_E^2 + Q^2 g_M^2}{4M^2 + Q^2} + \frac{Q^2}{4M^2} g_T^2 \right\},$$

where we have used the forms g_E , g_M

$$g_E = g_V - \mu \frac{Q^2}{4M^2}, \quad g_M = g_V + \mu$$

and g_E and g_M are found to have approximately the dipole form in electron scattering.

Data

The amount of experimental information on $\nu n \rightarrow \mu^- p$ is very limited and is indicated in the Table I. Hence we use theoretical guidance to reduce the number of parameters.

TABLE I

Determination of M_A from Neutrino Experiments

Experiment	Selected Events	Background	Flux Error	$M_A \pm \Delta M_A$ GeV	Reference
CERN Bubble Chamber	88	15%	$\pm 30\%$	0.75 ± 0.24	[1]
CF ₃ Br					
CERN Sp. Chamber	74	45%	$\pm 30\%$	0.65 ± 0.42	[2]
Al					
ANL Sp. Chamber	Few	25%	$\pm 30\%$	1.05 ± 0.20	[3]
Fe	Hundred				
CERN Bubble Chamber	26	10%	$\pm 15\%$	0.7 ± 0.2	[4]
C ₃ H ₈	66				
ANL Bubble Chamber	166	3%	$\pm 15\%$	0.95 ± 0.12	[5]
D ₂					

- (a) CVC— $g_s = 0$, $\mu = \mu_p - \mu_n$, Q^2 dependence given by electron scattering
- (b) g_p from pion pole dominance and hence giving a very small contribution
- (c) No second class currents, $g_T = 0$.

Hence the problem becomes one of determining the axial vector form factor g_A . Since we know $g_A(0)$ then if we put $g_A = \frac{g_A(0)}{(1 + Q^2/M_A^2)^2}$ (double pole form) then the only remaining variable is M_A .

Table I shows the results to date on M_A . The earlier experiments were all performed in complex nuclei (for reasons of event rate) and are therefore troubled by various nuclear problems — exclusion principle — final state interactions — confusion with $1-\pi$ channels etc. Nevertheless at the level of the statistics involved these problems are believed to be adequately understood and the experiments yield a value of M_A between 0.7–1.0 GeV.

A big step forward was taken with the exposure of the ANL 12-foot bubble chamber filled with deuterium to the neutrino beam. This experiment is still in progress but a result has been published [5] on the basis of 166 events.

Events are observed as:

$$\nu d \rightarrow \mu^- p(p_s) \quad \text{i.e. 2 or 3 prong.}$$

For 3 prongs this is a 3-C fit and for 2 prongs a quasi 3-C fit with P_s taken to be (0 ± 50) MeV/c in P_x, P_y, P_z .

The backgrounds were estimated at $(2 \pm 2)\%$ non ν and $(1 \pm 1)\%$ $\mu^- p \pi^0$ the latter being estimated on the basis of the observed $\pi^- \pi^+ p(p_s)$ events.

Before comparing with theory we must use a correction for low Q^2 loss because of the exclusion principle and for Fermi motion (only important for $Q^2 < 0.05$ (GeV/c) 2).

Fig. 1 shows σ_{total} and $d\sigma/dQ^2$ together with the best fits

$$\sigma_{\text{total}} \text{ gives } M_A = (0.94 \pm 0.18) \text{ GeV}/c^2 \text{ (needs flux 15\%)},$$

$$d\sigma/dQ^2 \text{ gives } M_A = (0.97 \pm 0.16) \text{ GeV}/c^2 \text{ (shape)},$$

overall $M_A = (0.95 \pm 0.12) \text{ GeV}/c^2$ (for comparison $M_V = 0.84 \text{ GeV}/c^2$).

As the data improves one will have to take into account relativistic corrections and the D-wave in the deuteron [6] ($\sim 5\%$ effects).

Test of CVC

As a crude test of CVC the ANL data has been fitted allowing M_A and M_V to vary. The best fit yields $M_V = 0.72^{+0.2}_{-0.14}$, $M_A = 1.15^{+1.2}_{-0.35} \text{ GeV}/c^2$ in satisfactory agreement with CVC.

Second Class Currents

To get some estimate of the magnitude of the effects a second class axial current might have on the elastic cross-section one might assume that the tensor coupling constant had the value $g_T \sim 3$ which would make it of intrinsic strength comparable to the weak magnetism ($\mu = 3.71$). One must in addition make some assumption about the Q^2 depen-

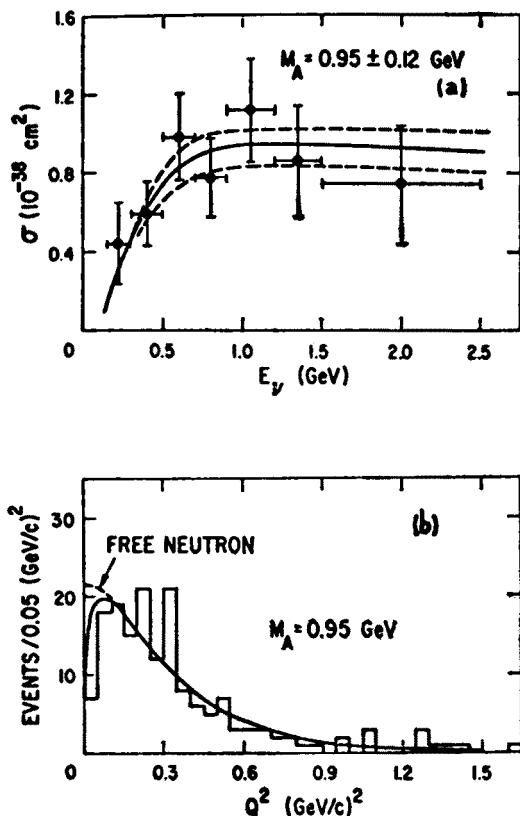


Fig. 1. The data from Ref. [5] on the process $\nu n \rightarrow \mu^- p$ (a) The total cross-section versus neutrino energy (b) The differential cross-section with respect to the four momentum transfer squared

dence of g_T and Tarrach and Pascual [6] have assumed a dipole form with $M_T^2 = 0.85$ and their resultant cross-section is shown in Fig. 2. It is clear that a 2nd class current of this magnitude would give clearly measurable effects in the cross-section. However, could one separate them from a variation in M_A or a departure from the dipole form for g_A ?

I think the answer is to use the maximum theoretical input and to see whether the data is consistent with the absence of 2nd class currents. To separate the effects of g_T and g_A one should determine

$$\left(\frac{d\sigma}{dQ^2} \right)_{\nu n} - \left(\frac{d\sigma}{dQ^2} \right)_{\bar{\nu} p},$$

since

$$\left(\frac{d\sigma}{dQ^2} \right)_{\nu n} - \left(\frac{d\sigma}{dQ^2} \right)_{\bar{\nu} p} = \frac{G^2 \cos^2 \theta_C}{4\pi M^2 E^2} (s-u) Q^2 g_A g_M,$$

taking g_M from CVC one can determine $g_A(Q^2)$.

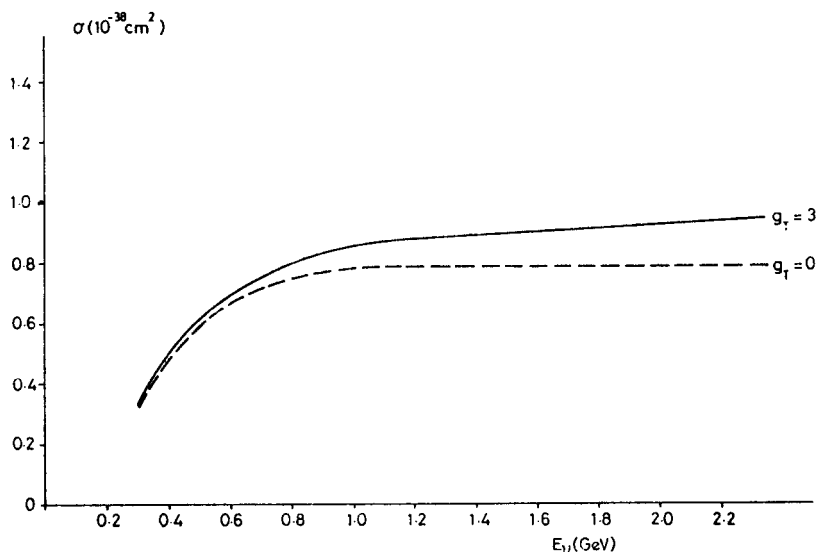


Fig. 2. The total cross-section for the process $\nu n \rightarrow \mu^- p$ as calculated by Tarrach and Pascual [6] including relativistic effects and D-wave in the deuteron. --- no tensor interaction, — including tensor interaction with $g_T = 3$

Then one can see whether σ_{total} has the form expected for this g_A . Clearly orders of magnitude more events are required than currently available. However the large bubble chambers at the new accelerators may supply them.

Polarization

Given large statistics at high energy it will be possible to measure the transverse polarization of the recoil proton (or neutron in $\mu^+ n$). This polarization is particularly sensitive to g_T . If we take the high energy limit then the polarization is given by

$$P = \frac{2 \sqrt{\frac{4M^2}{Q^2 + 4M^2}} \left\{ g_E g_A - \frac{Q^2}{4M^2} g_T g_M \right\}}{\left(g_A^2 + \frac{4M^2 g_E^2 + Q^2 g_M^2}{4M^2 + Q^2} + \frac{Q^2}{4M^2} g_T^2 \right)}.$$

Assuming all form factors have the same Q^2 dependence then P is shown in Fig. 3. It seems that a measure of the recoil polarization will be a sensitive test for the presence of 2nd class currents.

Δ -Production

The process $\nu p \rightarrow \mu^- \pi^+ p$ has been studied in two experiments: C_3H_8 CERN [7] 52 events (17% background) and H_2, D_2 ANL [8] 89 events.

The CERN experiment showed that $\Delta(1236)$ production dominated and obtained a plateau cross-section $E > 1$ GeV of $(1.13 \pm 0.28)10^{-38} \text{ cm}^2$.

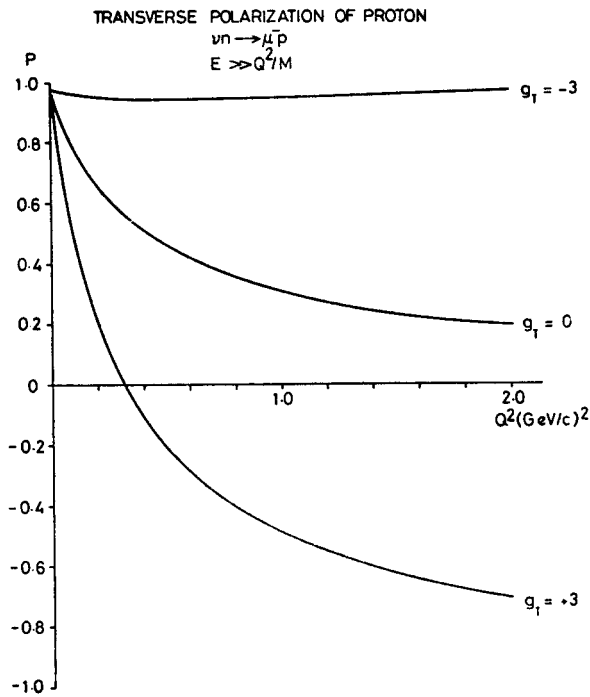


Fig. 3. The transverse polarization of the recoil proton in the process $\nu n \rightarrow \mu^- p$ at high energies. The effects of $g_T = 0$ or 3 are indicated

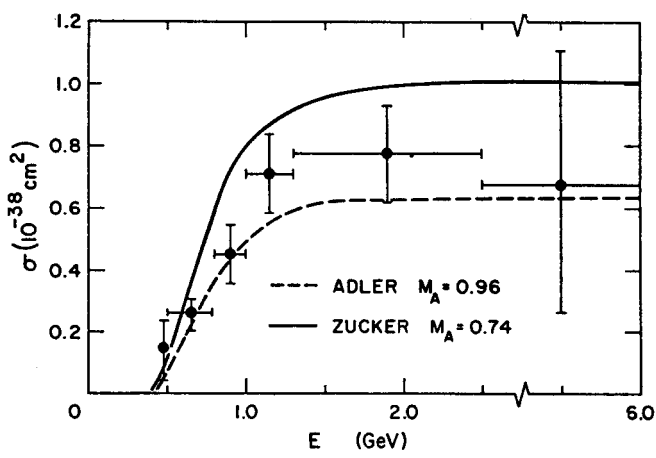


Fig. 4. Data from Ref. [8] on the total cross-section for the process $\nu p \rightarrow \mu^- \pi^+ p$ versus neutrino energy. — the best fit of the theory of Zucker [10] to σ and $d\sigma/dQ^2$. --- the similar best fit of the theory of Adler

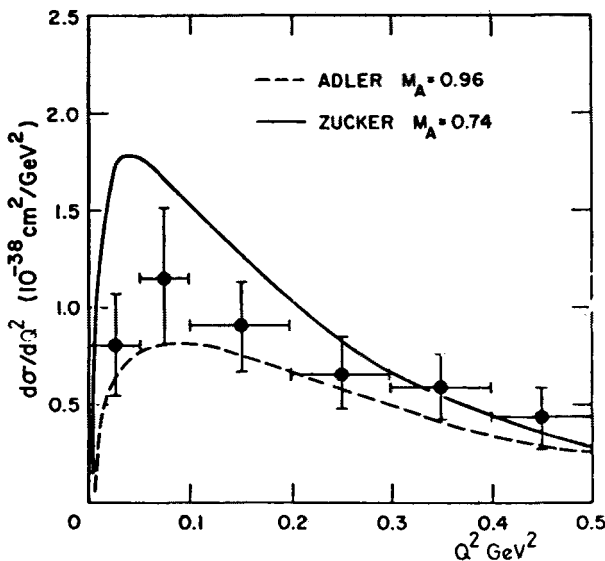
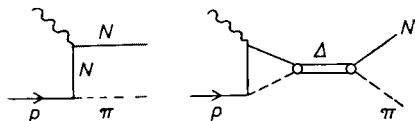


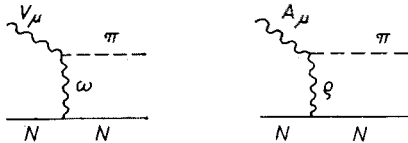
Fig. 5. Data from Ref. [8] on the differential cross-section for the process $\nu p \rightarrow \mu^- \pi^+ p$ with respect to the four momentum transfer squared; the curves are as in Fig. 4

The ANL experiment has so far reported on 189 events and find $\Delta(1236)$ accounts for $95 \pm 5\%$ of the final state. Total and differential cross-sections are shown in Figs 4 and 5. For $E > 1$ GeV, $\sigma = (0.74 \pm 0.18) \times 10^{-38}$ cm 2 i.e. somewhat lower than the CERN result.

These data have been compared with calculations based on the one-nucleon exchange Born terms enhanced by final state interactions,



Calculations of this type have been made by Adler [9] and by Zucker [10]. Adler includes the additional pion pole term and Zucker also ω and ϱ -exchange.



These calculations involve the current-nucleon coupling and hence g_A and M_A . The theories of Adler and Zucker differ in detail and, though both can fit the data they require different values of M_A

$$\begin{aligned} M_A &= 0.96 \text{ GeV}/c^2 && \text{Adler,} \\ &0.74 \text{ GeV}/c^2 && \text{Zucker.} \end{aligned}$$

A Test of the $\Delta I = 1$ Rule in Δ -production

This rule cannot be directly tested in β -decay. If the rule holds then

$$\langle \Delta^{++} | J | p \rangle = \langle \Delta | J | N \rangle,$$

$$\langle \Delta^+ | J | n \rangle = \frac{1}{\sqrt{3}} \langle \Delta | J | N \rangle,$$

hence $R = \frac{\sigma(\nu n \rightarrow \mu^- \Delta^+)}{\sigma(\nu p \rightarrow \mu^- \Delta^{++})} = \frac{1}{3}.$

This ratio would be 3 if $\Delta I = 2$ exchange were responsible for the interaction. Since a neutron target is required, this experiment must be performed in deuterium. The reaction

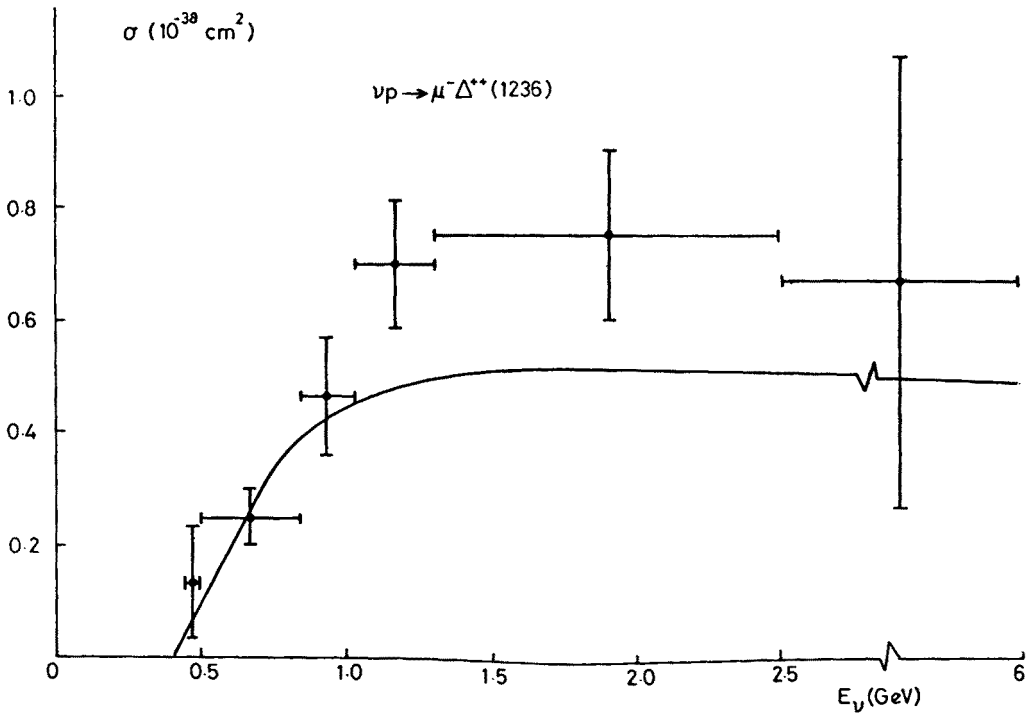


Fig. 6. The prediction of the quark model of Andreadis et al. [14] for the total cross-section for the process $\nu p \rightarrow \mu^- \Delta^{++}$ shown with the data of Ref. [8]

$\nu p \rightarrow \mu^- \Delta^{++}$ is easy to separate, however the Δ^+ reactions cannot be fitted since there is a neutral particle in the final state i.e. $\Delta^+ \rightarrow \pi^0 p, n\pi^+$. There is in fact a serious background from neutron interactions $nn \rightarrow \pi^+ \pi^- nn, \pi^- pn$ and from reactions due to incoming $\pi^\pm n \rightarrow \pi^\pm n$. Nevertheless an attempt at measuring R has been made by the ANL bubble chamber group [11]. Fourteen candidates for $\mu^- \pi^+ n$ were observed and 6 events of the type $\pi^- (\text{scatters}) \pi^+ n$. On the basis of the latter events it was estimated that 5 of the neutrino candidates were background. Hence from the 9 remaining events and the known branching

ratios it was estimated that

$$R = 0.32 \pm 0.2.$$

Also on the basis of two events with a μ^- decay plus a proton and associated (e^+e^-) pair (i.e. $\nu n \rightarrow \mu^- p \pi^0$) a second estimate was obtained

$$R = 0.36 \pm 0.28.$$

Clearly both estimates are consistent with $1/3$ but do not yet constitute a severe test of the $\Delta I = 1$ rule.

Higher Resonance Production — Quark Model

Recently there has been considerable work on applying the harmonic oscillator quark model to Δ and higher resonance production by neutrinos (Ravndal [12], Abdullah and Close [13], Andreadis et al. [14]).

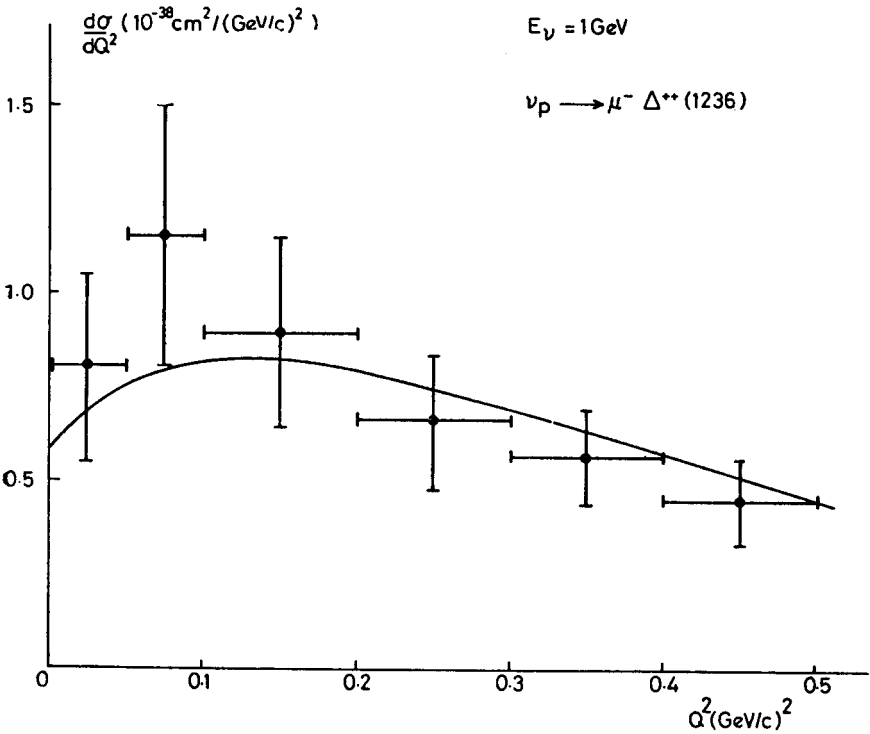


Fig. 7. As Fig. 6 for the differential cross-section $d\sigma/dQ^2$

These models assume that the weak hadron current is the sum of the quark currents and the lepton pair interacts with a single quark i.e.

$$H = \frac{G}{\sqrt{2}} \langle N^* | J_\mu | N \rangle j_\mu^{\text{lepton}}$$
$$J_\mu = \sum_i j_\mu^{\text{quark}(i)}$$

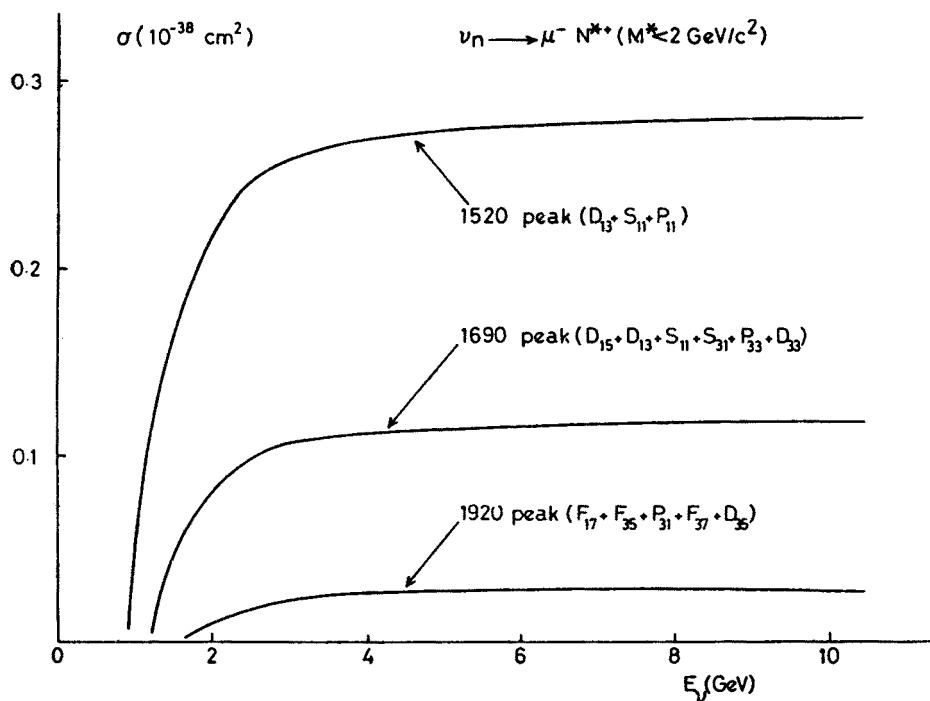


Fig. 8. The predictions of Andreadis et al. [14] for the cross-sections for the production of higher mass resonances in the process $\nu_n \rightarrow \mu^- N^{*+}$.

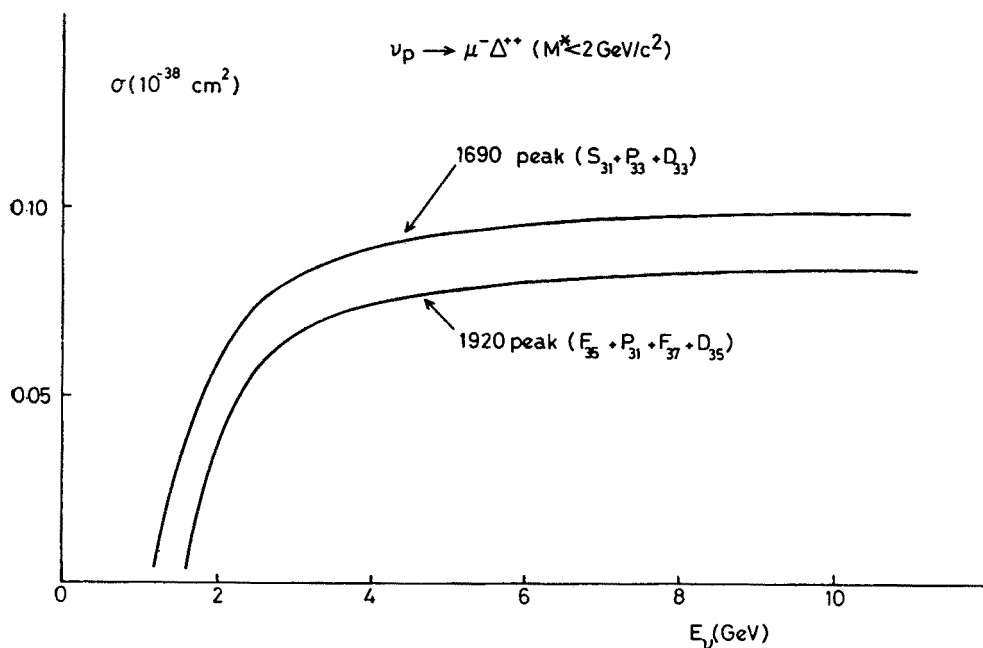


Fig. 9. As for Fig. 8 but for the $I = 3/2$ resonances produced in $\nu_p \rightarrow \mu^- \Delta^{*+}$

Hadron states are described by $SU(6)$ Harmonic Oscillator wave functions. These are basically non relativistic and relativistic effects are accounted for by

- (1) Modifying the quark mass equation
- (2) Introducing Dirac instead of Pauli spinors
- (3) Modifying the hadron state wave functions to take account of the finite momentum transfers.

In order to make predictions from the model we need to specify some parameters, e.g. axial vector coupling of the quarks — obtained from β -decay (vector couplings are obtained by CVC),

the harmonic oscillator radius of the nucleon — taken from Regge slope.

In addition in the model of Andreadis et al. the vector and axial vector form factors are obtained by assuming respectively ρ and A_1, π exchange dominance.

Hence using parameters fixed by external data the model can be used to predict total and differential neutrino cross-sections.

In Fig. 6 and Fig. 7 are shown the predictions of Andreadis et al. for σ and $d\sigma/dQ^2$ for $\Delta^{++}(1236)$ production and compared with the data from ANL. It can be seen that the predictions describe quite well the data and in fact they are approximately as good as fits of the dispersion relation models which were adjusted to the data using the free parameter M_A .

The virtue of the quark models appears to be that they can give predictions in a simple and direct way for the higher isobar production. In Fig. 8 and Fig. 9 are shown the predictions of Andreadis et al. for the higher N^* and Δ resonances. Bubble chamber experiments with the new accelerators at CERN and NAL should give data which will provide a quantitative test of the quark model.

REFERENCES

- [1] A. Orkin-Lecourtois, C. A. Piketty, *Nuovo Cimento* **50A**, 927 (1967).
- [2] M. Holder et al., *Nuovo Cimento* **57**, 338 (1968).
- [3] R. L. Kustom et al., *Phys. Rev. Lett.* **22**, 1014 (1969).
- [4] I. Budagov et al., *Lett. Nuovo Cimento* **2**, 689 (1969).
- [5] W. A. Mann et al., *Phys. Rev. Lett.* **31**, 844 (1973).
- [6] R. Tarrach, P. Pascual, *Nuovo Cimento* **18A**, 760 (1973).
- [7] I. Budagov et al., *Phys. Lett.* **29B**, 524 (1969).
- [8] J. Campbell et al., *Phys. Rev. Lett.* **30**, 335 (1973).
- [9] S. L. Adler, *Ann. Phys. (USA)* **50**, 189 (1968).
- [10] P. A. Zucker, *Phys. Rev.* **D4**, 3350 (1971).
- [11] ANL Bubble Chamber Group, Contribution to 6th International Symposium on Electron and Photon Interactions at High Energies, Bonn 1973.
- [12] F. Ravndal, *Lett. Nuovo Cimento* **3**, 631 (1972).
- [13] T. Abdullah, F. E. Close, *Phys. Rev.* **D5**, 2332 (1972).
- [14] P. Andreadis et al., *Orsay preprint* 74/5 (1974).

NEUTRAL CURRENTS

I. In this lecture I will review briefly the experimental developments since the Bonn Conference in 1973. For the situation at that time I would refer you to my review article published in the Proceedings of that Conference [1]. At present the positive results presented at Bonn still stand and they have been supported by increased statistics or improved analysis in some cases. In addition there are three new experimental results definitely indicating the presence of neutral currents in neutrino reactions.

II. The Process $\bar{\nu}_\mu e^- \rightarrow \bar{\nu}_\mu e^-$

This experiment [2] is being carried out in the Gargamelle heavy liquid bubble chamber at CERN. The signal for this process is an electron emitted at small angle to the neutrino beam

$$\theta_e \leq \sqrt{2m_e \left(\frac{1}{E_e} - \frac{1}{E_\nu} \right)} \quad \text{i.e. } 3.3^\circ \text{ at } 300 \text{ MeV.}$$

Therefore the selection criterion $E_e > 300 \text{ MeV}$, $\theta_e < 5^\circ$ were applied.

The running during the past year [3] has been carried out using the PS booster giving $5\text{--}6 \times 10^{12}$ ppp on the target. The events found so far are:

Sign	Energy (MeV)	$\theta_e [^\circ]$
—	385 ± 100	$1.4^{+1.6}_{-1.4}$
—	500 ± 120	2 ± 2
\pm or γ	1500 ± 500	< 2
+	~ 2000	5.5
+	3000 ± 1000	5.0 ± 0.5

The only significant sources of background are believed to be:

1) $\nu_e n \rightarrow e^-(p)$, $\theta_e < 5^\circ$, proton not seen, from ν_e contamination in the beam. This background can be reliably estimated from the similar reaction

$$\nu_\mu n \rightarrow \mu^-(p), \quad \theta_\mu < 5^\circ,$$

which is observed. The ν_e flux in antineutrino is only known by calculation, however the corresponding ν_e flux in neutrino checks with the observed number of events with electrons.

2) Isolated γ -rays can give background if they materialise as Compton electrons or asymmetric pairs. This background also can be reliably estimated from the number and angular distribution of isolated γ 's giving (e^+e^-) pairs.

The total background in the antineutrino running is calculated to be $(0.14 \pm .09)$ events whereas, as we see, two have been observed. As a fluctuation based on Poisson statistics this has a probability of $< 2\%$.

The number of small angle e^+ events (interpreting the dubious event as an e^+) is compatible with the expected number from

$$\bar{\nu}_e p \rightarrow e^+(n).$$

This number can be estimated from 22 events of the type $\bar{\nu}_\mu p \rightarrow \mu^+ n$, $\theta_\mu < 5^\circ$ found in a sample of the film and the flux ratio $\bar{\nu}_e/\bar{\nu}_\mu = 0.7\%$. It is found that 2-3 events would have been expected.

A detailed comparison with theoretical expectations will have to wait until the complete data on the present series of runs has been accumulated. However if we look at the process in the Salam-Weinberg theory we find an effective Hamiltonian

$$\begin{aligned} H_{\text{eff}} &= \frac{g+g'}{16m_Z^2} [(4 \sin^2 \theta_W - 1) \bar{e} \gamma_\mu e - \bar{e} \gamma_\mu \gamma_5 e] [\bar{\nu}_\mu \gamma_\mu (1 + \gamma_5) \nu_\mu] = \\ &= - \frac{G}{2\sqrt{2}} [\bar{\nu}_\mu \gamma_\mu (1 + \gamma_5) \nu_\mu] [\bar{e} \gamma_\mu (g_V + g_A \gamma_5) e], \end{aligned}$$

where

$$\frac{G}{2\sqrt{2}} = \frac{g^2 + g'^2}{16m_Z^2}, \quad g_V = \frac{1}{2} - 2 \sin^2 \theta_W, \quad g_A = \frac{1}{2}.$$

The differential cross-section calculated from this H_{eff} has been given by t'Hooft [4]

$$\frac{d\sigma}{dE_e} = \frac{G^2 m_e}{2\pi} \left[(g_V + g_A)^2 + (g_V - g_A)^2 \left(1 - \frac{E_e}{E_\nu}\right)^2 + \frac{m_e E_e}{E_\nu^2} (g_A^2 - g_V^2) \right].$$

Hence given the neutrino flux, we can calculate the expected yield of events with $E_e > 300$ MeV. The minimum number of events occurs for $\sin^2 \theta_W \sim 0.1$ and corresponds to 1.9 events for the running completed to date. Two events are observed so the experiment is certainly compatible with the theory.

III. Inclusive Semi-leptonic Neutral Currents

This class of experiments looks for the process

$$\nu N \rightarrow \nu X.$$

(a) Gargamelle Experiment at CERN

The types of event searched for are represented schematically in Fig. 1. The principal source of background is believed to be neutrons generated by neutrino interactions in the material surrounding the bubble chamber. This type of background was estimated on the observed AS events and was found to account for only $\sim 20\%$ of the observed "muonless" events. After subtracting this background the ratio of neutral to charged current cross-

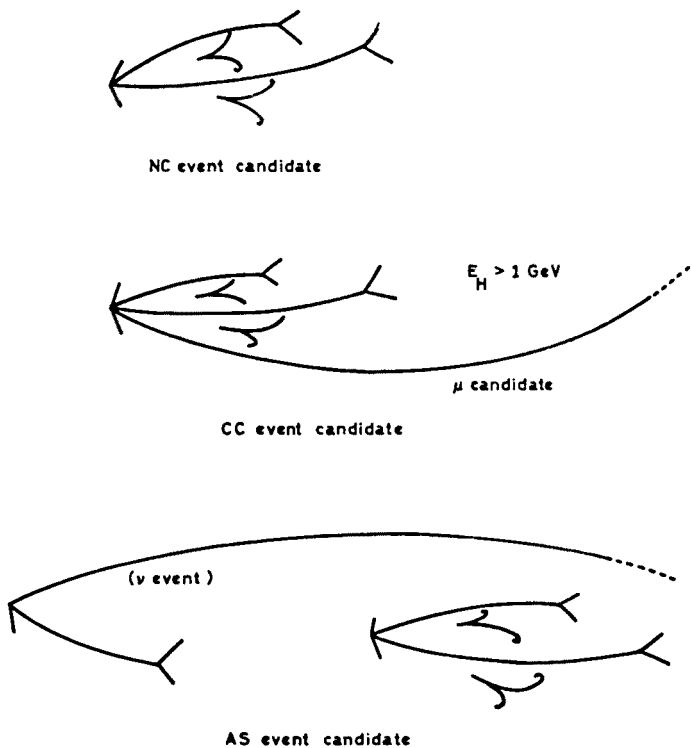


Fig. 1. Definitions of the event types searched for in the Gargamelle experiment [5] on semileptonic neutral currents

sections was found to be [5]

$$\left(\frac{\text{NC}}{\text{CC}}\right)_\nu = 0.22 \pm 0.04, \quad \left(\frac{\text{NC}}{\text{CC}}\right)_{\bar{\nu}} = 0.43 \pm 0.12.$$

These results could be criticized on the grounds that the number of AS events was small and that some of the crucial parameters of the neutron cascade Monte Carlo were not determined by experiment.

In answer to the first point, more film has been measured and the status as of the Philadelphia meeting [6] is:

September 1973	April 1974
$\text{NC}/\text{film} \begin{cases} \nu & 102/111 = 0.92 \pm 0.13 \\ \bar{\nu} & 63/276 = 0.23 \pm 0.03 \end{cases}$	$\begin{aligned} 191/197 &= 0.97 \pm 0.10 \\ 70/298 &= 0.235 \pm 0.030 \end{aligned}$
$\text{AS}/\text{film} \begin{cases} \nu & 15/111 = 0.135 \pm 0.037 \\ \bar{\nu} & 12/276 = 0.043 \pm 0.012 \end{cases}$	$\begin{aligned} 40/277 &= 0.144 \pm 0.025 \\ 14/328 &= 0.042 \pm 0.012 \end{aligned}$

The conclusion is that the increased statistics ($\times 2$ for the AS events) has not changed the estimates of the rate of occurrence of NC and AS events.

In order to improve the input to the neutron Monte Carlo, Gargamelle has been exposed to proton beams of 4, 7, 12 and 19 GeV/c. It would be expected that the behaviour

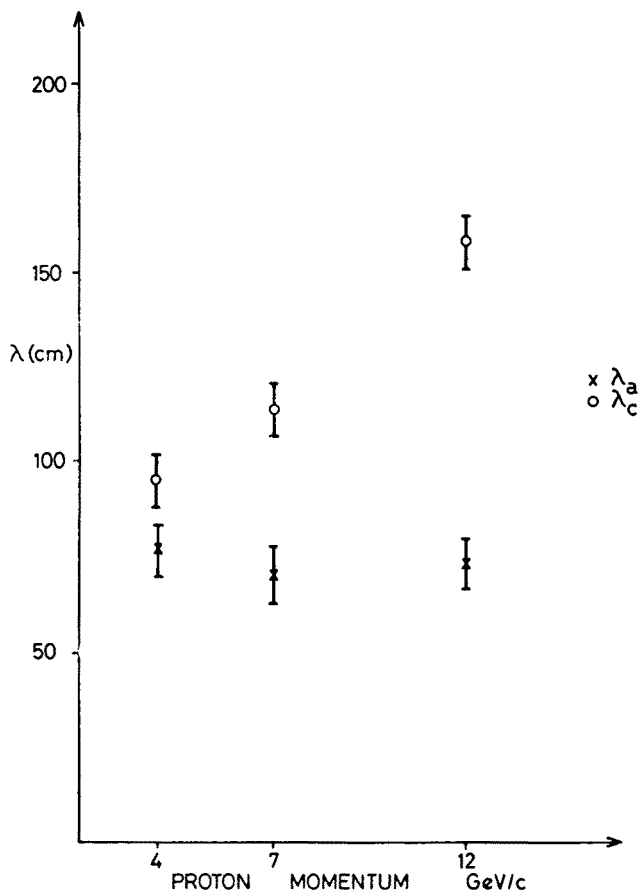


Fig. 2. Results on λ_a and λ_c as defined in the text obtained from an exposure of Gargamelle to proton beams of 4, 7 and 12 GeV/c

of protons should be very similar to that of neutrons in CF_3Br . Two of the crucial parameters are

λ_a — the average length to the first interaction to deposit more than 150 MeV;

λ_c — the cascade length i.e. the average length a proton may travel before the last interaction in which it deposits > 1 GeV.

The data on λ_a and λ_c are shown in Fig. 2. If these values are inserted in the Monte Carlo they confirm that $B/AS \sim 0.7$.

Another interesting aspect of the data which has been studied is the charge ratios of the pions produced in CC, NC, and AS events. The following ratios are found, combining ν and $\bar{\nu}$ events with equal weight:

	$\pi^0/(\pi^+ + \pi^-)$	π^0/π^-
CC	0.83 ± 0.08	2.14 ± 0.24
NC	0.68 ± 0.06	1.72 ± 0.29
AS	0.26 ± 0.09	0.61 ± 0.27
NC-CC	-0.15 ± 0.10	-0.42 ± 0.37
NC-AS	$+0.42 \pm 0.11$	1.11 ± 0.40

The table shows that the charge ratios of NC and CC events are compatible, particularly if one allows for a $\sim 20\%$ neutron background, whereas NC and AS are significantly different. This is independent evidence that the AS and NC events have different origins.

(b) Experiment 1A at NAL

This is the Harvard-Pennsylvania-Wisconsin-NAL experiment and so far they have published data from three separate runs [7], [8], [9].

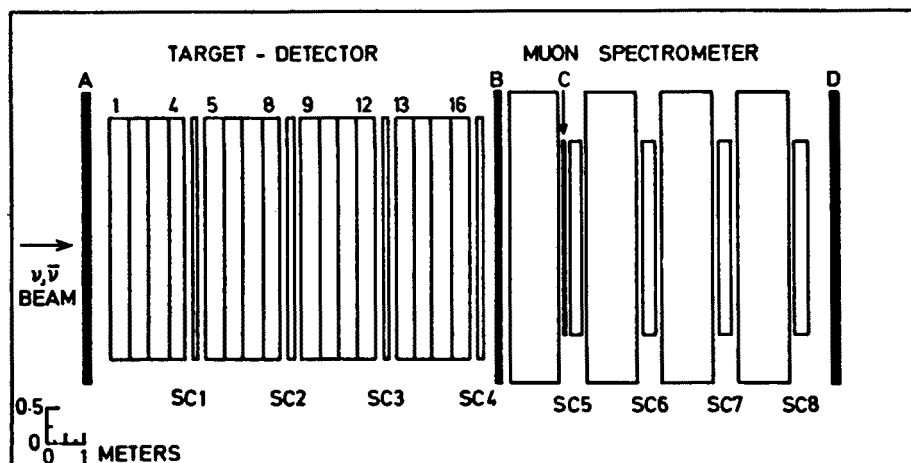


Fig. 3. The apparatus used by Benvenuti et al. [7] for their first neutral current search

(i) This experiment was performed using the apparatus shown in Fig. 3. It consists of a 70-ton calorimeter of liquid scintillator, split into 16 segments. The energy of the hadronic shower is measured by pulse height to $\pm 15\%$ and the signs and momenta of muons are determined in a magnetized iron spectrometer consisting of 4 sections each 1.5 m long. Four wide-gap spark chambers are placed between the modules of the calorimeter and

four narrow gap chambers within the magnet. The signals for events without and with muons are:

“muonless” $\bar{A} E \bar{C}$ (No SC5),
 with muon $\bar{A} E B$ (C or SC5).

E is a signal in the calorimeter and events were selected in which $E > 6$ GeV at proton energy of 300 GeV and $E > 13$ for proton energy 400 GeV. Events were accepted in a fiducial region consisting of a 2.0×2.0 m² transverse area of calorimeter modules 7–12. The run yielded 93 events with a muon and 76 “muonless” events. However the “muonless” events contained events in which a muon was present but missed counter C. This correction was calculated on the basis of the events observed in the calorimeter and the first magnet

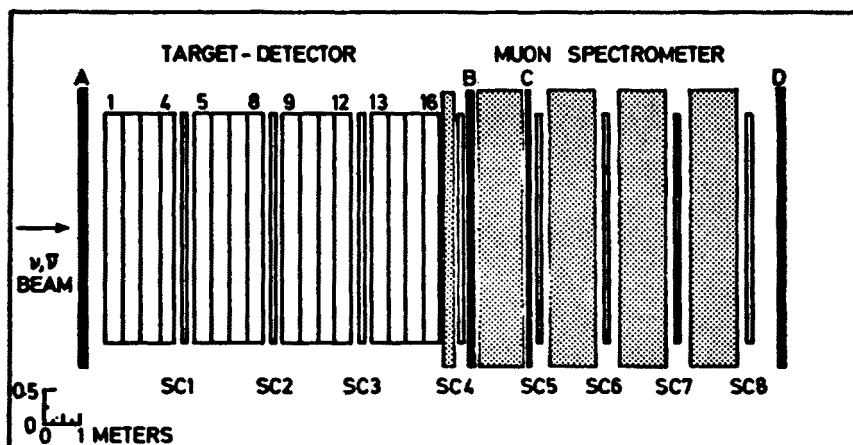


Fig. 4. The apparatus used by Aubert et al. [8], [9] for their later experiments. This apparatus differs from that in Fig. 3 in having a greater muon detection efficiency for neutrino events in the calorimeter

section, and assuming azimuthal symmetry and a uniform vertex distribution. It was found that of the 76 “muonless” events 38 would contain an undetected muon. Hence $NC/CC = 0.29 \pm 0.09$.

In fact a note added in proof [7] takes account of the effect of spatial reconstruction errors on the muon detection efficiency and gives a revised $NC/CC = 0.23 \pm 0.09$. Note that this result is for a beam which consists of 80% ν and 20% $\bar{\nu}$.

(ii) In this run [8] the apparatus above was modified as in Fig. 4 to give a greater muon acceptance. This was achieved by adding 35 cms of iron upstream of SC4 so that SC4 and counter B could be used for muon identification. Furthermore the area of counter C was increased and the spark chambers in the magnet were replaced by wide-gap types. These changes bring the average muon detection efficiency to $\sim 85\%$. This is shown in Fig. 5c.

However, a correction now has to be applied for hadrons which “punch through” the relatively thin absorber and simulate muons. This effect is determined from events

with a clear muon in counter C and an additional track in (B or SC4). This punch through correction is shown as a function of vertex position and hadronic energy in Figs. 5a and 5b.

The beam was produced by 300 GeV protons on an aluminium target and secondary pions and kaons were focussed by a magnetic horn to give a beam enriched in antineutrinos. The ratio α of events with a μ^- to the total was observed to be $\alpha = \mu^-/(\mu^+ + \mu^-) = 0.63 \pm 0.11$.

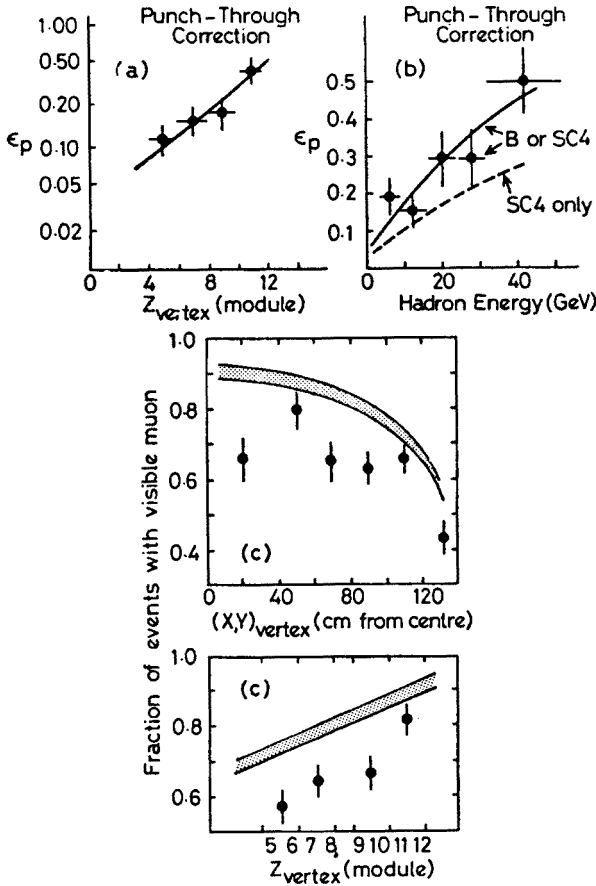


Fig. 5. (a) The “punch through” correction ϵ_p as a function of the Z-position of the vertex of the neutrino interaction; (b) ϵ_p as a function of the hadron energy released in the interaction; (c) The observed fraction of events with a muon as a function of Z and (X, Y) after correction for hadron punch through. The data shown was obtained using SC4 as muon identifier

A total of 535 events were observed in segments 5–12 of the calorimeter and with an energy deposition greater than 4 GeV. The observed ratio R_M of events without a muon to those with a muon is related to $R = NC/CC$ by

$$R = \frac{NC}{CC} = \frac{(\epsilon_\mu + \epsilon_p - \epsilon_\mu \epsilon_p)(1 + R_M)}{1 - \epsilon_p(1 + R_M)}.$$

Figs 6a, 6b, 6c show R as a function of spatial position of the vertex and of the hadron energy E_H . The data are consistent with a constant value:

$$R = 0.20 \pm 0.05.$$

Since the beam is a mixture of ν and $\bar{\nu}$ we have

$$R = \alpha R_\nu + (1 - \alpha) R_{\bar{\nu}}$$

and this is shown in Fig. 6d. It clearly excludes a null result i.e. no neutral current by about 4 standard deviations.

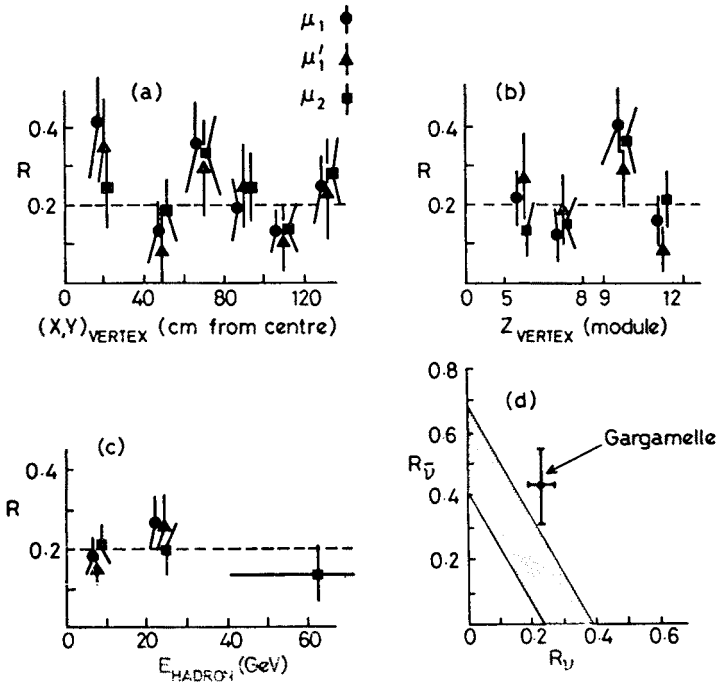


Fig. 6. The variation of the ratio R with: (a) the (X, Y) position of the interaction vertex, (b) the Z -position of the vertex, (c) the hadron energy deposited in the interaction. Data are shown for three muon identifiers: μ_1 — B or SC4, μ'_1 — SC4, μ_2 — C or SC5, (d) the allowed region of R_ν and $R_{\bar{\nu}}$; the Gargamelle result is also shown

A more refined analysis has been made [9] by taking into account the variation of beam composition during the spill, since the horn pulse was shorter than the proton beam duration. This is shown in Fig. 7. The data can be grouped into a central region with $\alpha = 0.45 \pm 0.06$ and to the remainder with $\alpha = 0.74 \pm 0.06$. The corresponding values of R are:

$$\begin{aligned} \alpha &= 0.74 \pm 0.06 & R &= 0.18 \pm 0.05, \\ \alpha &= 0.45 \pm 0.06 & R &= 0.22 \pm 0.05. \end{aligned}$$

Hence we can solve for R_ν and $R_{\bar{\nu}}$ and the result is shown by the elliptical region in Fig 8.

(iii) Finally the apparatus described in (ii) was operated [9] in the dichromatic neutrino and antineutrino beams which have much greater purity. The mean energy was ~ 50 GeV and the corresponding values of α were $\alpha = 0.12 \pm 0.05$ ($\bar{\nu}$ beam) and $\alpha = 0.98 \pm 0.01$ (ν beam). The results were $R_\nu = 0.13 \pm 0.06$, $R_{\bar{\nu}} = 0.34 \pm 0.12$.

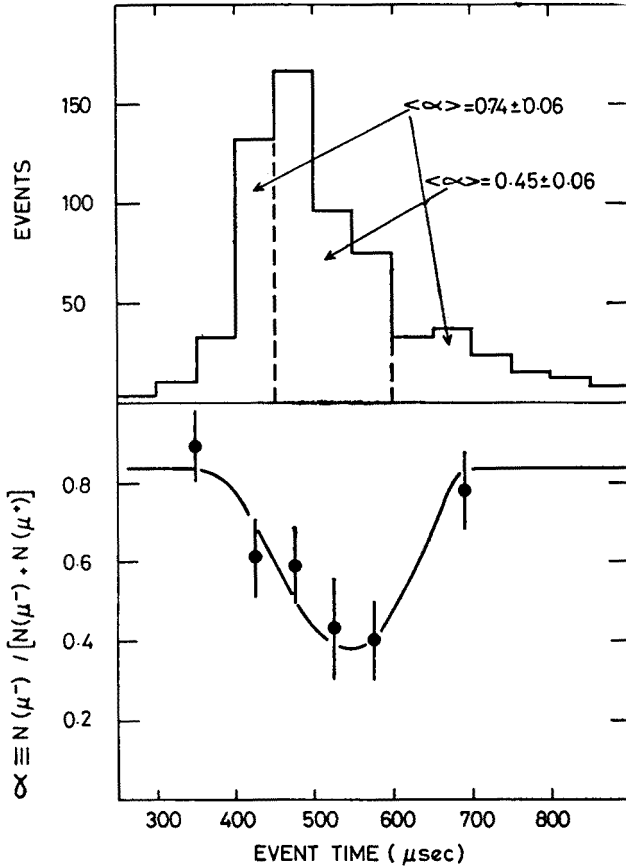


Fig. 7. Time distribution of the neutrino events and the ratio α during the beam pulse

A fit of the results (ii) with spill time analysis and (iii) give $R_\nu = 0.11 \pm 0.05$, $R_{\bar{\nu}} = 0.32 \pm 0.09$.

These results are shown in Fig. 9 together with the Gargamelle result. Also shown is the lower limit calculated by Paschos and Wolfenstein [10] and Pais and Treiman [11] from Salam-Weinberg theory assuming $V = A$ and neglecting the isoscalar contribution. A correction to the theory for the selection criteria is shown for the Gargamelle data. Some correction will be necessary for the Experiment 1A but will probably be smaller.

The following remarks seem appropriate:

The NAL results for R_ν and $R_{\bar{\nu}}$ are lower than those found at CERN but not incompatible ($\sim 1.5\sigma$);

Both sets of data suggest a value of $\sin^2 \theta_w$ in the range 0.3–0.5; The NAL results are consistent with equal neutral cross-sections for ν and $\bar{\nu}$, although the Gargamelle results would exclude this possibility.

IV. Single Pion Production by Neutral Current

This experiment [12] was performed in the ANL 12-foot bubble chamber filled with hydrogen (300,000 pulses) and deuterium (600,000 pulses). This exposure corresponded

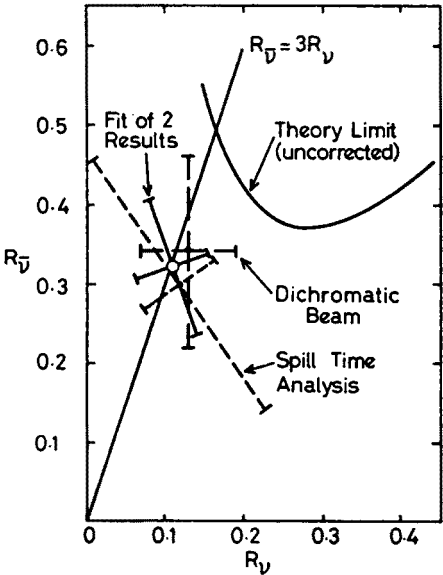
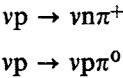


Fig. 8. The results of experiment (ii) with spill time analysis and (iii) the dichromatic beam experiment together with a fit to both sets of results

to a total of 4×10^{17} protons of 12 GeV on target. The following reactions were sought in the 11.1 m³ fiducial volume



and compared with the events of the type $\nu p \rightarrow \mu^- p \pi^+$.

(i) $\nu n \pi^+$. The signature for this interaction is a single positive pion. Tracks were identified as pions by:

- (a) A clear $\pi \rightarrow \mu \rightarrow e$ decay on a stopping track.
- (b) A kinematically fitted $\pi^+ p$ elastic scatter.
- (c) Energy loss on low-momentum leaving tracks.

The following selections were applied to 18 candidates found:
 $p_{\pi} < 400$ MeV/c. This was to give good discrimination by method (c);

The dip angle $\lambda < 0$. Incoming neutrons can simulate neutral current events in the reaction $np \rightarrow nn\pi^+$. The charge symmetric reaction $np \rightarrow pp\pi^-$ is observed (12 events) and it is found that 90% of the neutrons and π^- are directed downwards ($\lambda > 0$) indicating that the neutrons are entering by the weakly shielded top of the chamber; The event must be > 20 cms away from any cosmic ray track. This was to remove background from the reaction $\gamma p \rightarrow \pi^+ n$ with γ produced by a cosmic ray.

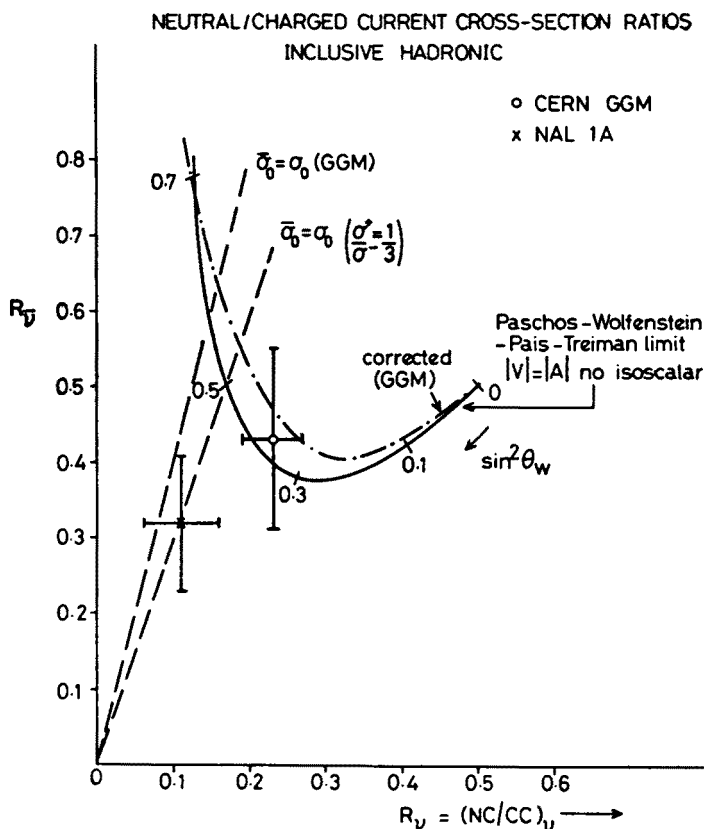


Fig. 9. The overall fit to the results of experiment 1A shown together with the Gargamelle result. The dashed lines indicate the variation of $R_{\bar{\nu}}$ versus R_{ν} if the neutral current cross-sections contained no V-A interference ($\sigma_0 = \bar{\sigma}_0$). Two lines are shown corresponding to a charged cross-section ratio of 1/3 and to that actually measured in the Gargamelle experiment, including the effects of experimental biases. The dashed-dotted curve shows the effect of the biases in the Gargamelle experiment on the theoretical limit

The effect of all selections was tested on the sample of $\mu^- p \pi^+$ events. After these selections 7 events were left. The remaining backgrounds were estimated to be:

neutrons	0.55 ± 0.55
γ -induced	0.33 ± 0.10
$\bar{\nu} p \rightarrow \mu^+ n$	0.04 ± 0.04
Total	0.92 ± 0.56

(ii) $\nu p \pi^0$. The signature for this reaction was an (e^+e^-) pair pointing to the origin of a proton track. Thirteen events were found and the following selection criteria were applied:

The dip, λ , and azimuthal, φ , angles of the proton were both $< 60^\circ$. It was found that 99% of $\mu^- p \pi^+$ events satisfied this criterion;

Proton momentum $< 1 \text{ GeV}/c$. 91% of $\mu^- p \pi^+$ events satisfied this criterion;

Vertex $> 20 \text{ cms}$ from a cosmic ray.

After applying these criteria 7 events were left. The remaining backgrounds were estimated to be:

neutrons	0.92 ± 0.40
γ -induced	0.02 ± 0.01
Accidentals	0.11 ± 0.11
Incoming $\pi^- p \rightarrow \pi^0 n$	0.52 ± 0.23
Total	1.57 ± 0.47

In this case the neutron background estimate was based upon the observed number of $pp\pi^-$ events and the ratio $\gamma p/pp\pi^- = 0.19 \pm 0.04$ determined in a separate exposure to a neutron beam.

Hence the overall result is a total of 14 events with an estimated background of 2.49 events. As a statistical fluctuation this has a probability corresponding to about 4σ .

The ratios to the charged current single pion production are

$$R_0 = \frac{\sigma(\nu p \rightarrow \nu p \pi^0)}{\sigma(\nu p \rightarrow \mu^- p \pi^+)} = 0.48 \pm 0.25,$$

$$R_+ = \frac{\sigma(\nu p \rightarrow \nu n \pi^+)}{\sigma(\nu p \rightarrow \mu^- p \pi^+)} = 0.17 \pm 0.08.$$

Hence $R_0 + R_+ = 0.65 \pm 0.27$. Recently Adler [13] has calculated the limits $0.15 < R_0 + R_+ < 0.44$ based on Salam-Weinberg Theory. The Argonne result is higher than, but not inconsistent with this prediction. The result also gives the charge ratio of the pions produced by the neutral current:

$$\frac{\nu p \rightarrow \nu p \pi^0}{\nu p \rightarrow \nu n \pi^+} = 2.9 \pm 2.0.$$

A value of 2 would correspond to $I = 3/2$ dominance of the final state and this is favoured by the data, although a value of $1/2$ corresponding to $I = 1/2$ final state cannot be ruled out. If the neutral current were uniquely isoscalar then only $I = 1/2$ states would be allowed.

V. Conclusions

The experimental progress over the last year appears to have established beyond doubt the existence of neutral weak currents. However, the fundamental properties of these currents remain to be determined. For example:

what is the V, A composition of the neutral currents involved in leptonic and semi-leptonic reactions?

what is the isospin structure of the hadronic neutral current?

are the leptonic and semileptonic reactions consistent with Salam-Weinberg theory?

If so what is the value of θ_w ? Is it the same for leptons and hadrons?

It will clearly be necessary to carry out a long series of sophisticated experiments before these features of this new phenomenon are established.

REFERENCES

- [1] G. Myatt, Neutral Currents, *Proceedings of the 6th International Symposium on Electron and Photon Interactions at High Energies*, Bonn 1973.
- [2] F. J. Hasert et al., *Phys. Lett.* **46B**, 121 (1973).
- [3] F. J. Hasert et al., reported in the Review talk of A. Rousset, International Conference on Neutrino Physics and Astrophysics, Philadelphia 1974.
- [4] G. t'Hooft, *Phys. Lett.* **37B**, 195 (1971).
- [5] F. J. Hasert et al., *Nucl. Phys.* **B73**, 1 (1974).
- [6] F. J. Hasert et al., reported in the Review talk of A. Rousset, (See Ref. [3]).
- [7] A. Benvenuti et al., *Phys. Rev. Lett.* **32**, 800 (1974).
- [8] B. Aubert et al., *Phys. Rev. Lett.* **32**, 1454 (1974).
- [9] B. Aubert et al., *Phys. Rev. Lett.* **32**, 1457 (1974).
- [10] E. A. Paschos, L. Wolfenstein, *Phys. Rev.* **D7**, 91 (1973).
- [11] A. Pais, S. B. Treiman, *Phys. Rev.* **D6**, 2700 (1972).
- [12] S. Barish et al., reported at the meeting of the American Physical Society, Washington, 1974.
- [13] S. L. Adler, *Phys. Rev.* **D9**, 229 (1974).